University of Hertfordshire UH

PROJECT REPORT

BEng Aerospace Engineering

Name: Abel Virtue Ochieng

Supervisor: Dr Matt Goodro

Stability and Configuration Study on Amphibious Quadcopter Drones – Aerial Expert

Date: 22nd March 2024

BACHELOR OF ENGINEERING DEGREE/DEGREE WITH HONOURS IN AEROSPACE ENGINEERING

Department of Engineering
School of Physics, Engineering and Computer Science
University of Hertfordshire

STABILITY AND CONFIGURATION STUDY ON AMPHIBIOUS QUADCOPTER DRONES – AERIAL EXPERT

Report by
Abel Virtue
Ochieng

Supervisor
Dr Matt Goodro

Date
22nd March 2024

DECLARATION STATEMENT

I certify that the work submitted is my own and that any material derived or quoted from the published or unpublished work of other persons has been duly acknowledged (ref. UPR AS/C/6.1, Appendix I, Section 2 – Section on cheating and plagiarism).

I confirm that any study conducted as part of my project that involved human participants has been approved in accordance with UH Ethical regulations and the protocol number(s) is/are:

LIST ANY ETHICAL APPROVAL REFERENCE NUMBERS HERE OR TYPE “N/A” IF NOT APPLICABLE

Student Full Name: Abel Ochieng

Student Registration Number: 20011451

Signed: Abel Ochieng

Date: 22nd March 2024

ABSTRACT

An amphibious quadcopter is a vehicle capable of moving through air and water. Drag is a critical force that affects the performance of a quadcopter during operation. There are several factors that contribute to drag on a quadcopter including the shape and arm configuration of the quadcopter. This project focuses on evaluating the aerodynamic performance of common quadcopter configurations using Computational Fluid Dynamics (CFD) simulations to investigate the drag force experienced by different quadcopter models moving through air.

The study begins by developing 3D models of four commonly used quadcopters and thereafter conducting CFD simulations on the models to obtain aerodynamic drag values of the models. From the drag values, the coefficients of drag for each configuration will be determined and compared. Based on these results, a recommendation of the most aerodynamic configuration will be made. The aerodynamic results will also be compared to hydrodynamic results and a recommendation of the optimal configuration for an amphibious quadcopter will be made. Findings suggest that the quadcopter in the shape of an X performs better in both environments in comparison to other configurations.

Areas for improvement and future work will be identified to further aid the development of the project by considering structural integrity in addition to fluid dynamics.

ACKNOWLEDGEMENTS

I would like to express my appreciation and gratitude to Dr Matt Goodro for guiding, helping and providing me with relevant resources through the entirety of the project.

In addition, I would like to thank my family and friends for their unwavering support and encouragement in completing this project.

Lastly, I would like to thank my classmates who have helped me in one way or the other as we navigate through the ups and downs of our undergraduate studies.

TABLE OF CONTENTS

LIST OF FIGURES

LIST OF EQUATIONS

GLOSSARY

Acronyms

CAD – Computer Aided Design

CAE – Computer Aided Engineering

CFD – Computational Fluid Dynamics

ISA – International Standard Atmosphere

UAV – Unmanned Aerial Vehicle

VTOL – Vertical Take Off and Landing

Units

kg – Kilogram

kg/m^3 – Kilogram per cubic meter

mph – Miles per hour

m/s – metre per second

Pa - Pascal

Pa•s – Pascal second

Software used and their abbreviations.

CATIA – Computer Aided Three-Dimensional Interactive Application. CAD and CAE software used to design models and engineering drawings.

Excel – Microsoft spreadsheet editor used for calculating and computation purposes.

MATLAB –programming and numeric computation software used to analyse data, develop algorithms and develop models.

Star CCM+ - Computer software used to perform the CFD simulations.

Vocabulary

Mesh – a network formed of cells and points that divides a geometry into many elements

Meshing – the process of generating mesh cells.

1. Introduction

A quadcopter is an unmanned aerial vehicle with four motors and propellers. Over the last years, the use of UAV's has become common in the military, civilian and industrial sectors. They are widely used for aerial photography, surveillance, land surveys, weather broadcasting, search and rescue, agriculture marine studies and wildlife monitoring.

Figure 1 A quadcopter used in agriculture to spray water and pesticides on crops. [2]

One of the important elements in the design of a quadcopter is stability. A stable quadcopter is able to maintain its flight path and return to its original flight path following a small perturbation like crosswind. Weight, wind, currents, quadcopter arm configuration and rotor vibrations are among the factors that affect the stability of a quadcopter. Quadcopter arm configuration refers to the shape and arrangement of the arms on a quadcopter. It plays a major role in the fluid dynamics of the quadcopter. The more fluid dynamic a quadcopter is, the easier it is to move through air with minimal drag and resistance, making the quadcopter more efficient and less energy consuming. The commonly used configurations include True X, Plus, H and Hybrid X. Each configuration results in different fluid dynamic behaviours for the quadcopter.

1.1 Project Background

An amphibious quadcopter is a drone that can operate both in air and water. Since air and water are fluids with different physical properties such as density and viscosity, the performance of an amphibious quadcopter will be different in both fluids. While designing an amphibious quadcopter, an engineer must consider the effect of both air and water on the drone. For example, all electronic components must be protected either by being stored inside the drone or by having a protective covering that will keep the water out. The quadcopter should be able to resist aerodynamic forces, hydrodynamic forces and the varying pressure acting on it in both fluids.

Regardless of the fluid a quadcopter moves through, its stability is a key component. This project investigates how the aerodynamics of a quadcopter flying in air is affected by the different configurations of the quadcopter.

1.2 Project Aim

The aim of the project is to evaluate the performance of common quadcopter configurations in aerial environments by investigating drag values using CFD.

1.3 Project Objectives

1. Design quadcopter models with different configurations that are commonly used, using CATIA v5 by Dassault Systems.
2. Conduct CFD simulations of the quadcopter models using Star CCM+, developed by Siemens Digital Industries.
3. Investigate and compare the performance of the models at different velocities and assess their drag values.

1.4 Project Report Structure

This report consists of 10 sections in the following order:

1. Introduction
2. Literature Review
3. CAD Modelling
4. CFD Methodology
5. Validation
6. Results
7. Conclusion
8. Further Development
9. Project Management Review
10. Quality Management

2. Literature Review

This section is a review of the background and development of amphibious quadcopters with a focus on the quadcopter flying in air.

2.1 History of Quadcopters

Quadcopters were first created in the early 1900's as a solution for the problems faced during vertical take-off and landing (VTOL) flight in helicopters [3]. Among the first quadcopters to be created was the Gyroplane No.1 designed by the Breguet brothers in 1907 [1]. The quadcopter had a seat for the pilot and a power plant at the centre that drove the four rotors.

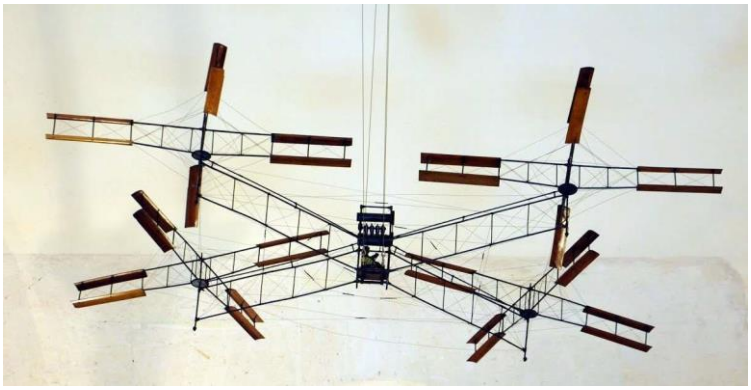

Figure 2 Gyroplane No 1 designed by the Breguet brothers.

Following this invention, various early quadcopters were designed and built that followed the same design principles as the Gyroplane No.1. Early quadcopters typically had the engine at the centre of the fuselage driving the four rotors using shafts or belts. This meant that the 4 rotors were run at the same speed and had to produce enough lift to remain airborne. This resulted in unstable flights and the absence of advanced computers and motors lead to work overload on the pilot to stabilise the quadcopter.

The development of advanced computers, electric motors and microelectronics, made it possible to design and build efficient and reliable quadcopters with the ability to maintain stability. In modern quadcopters, each rotor is fitted with its own electric motor which made it possible to operate the rotors at different speeds. This enabled the quadcopter to be operated and controlled without a pilot, hence the reason why it is classified as unmanned. This also allowed for the size of quadcopters to be reduced, modern quadcopters can be as small as the size of an adult human palm. Basic operation principles of modern quadcopters are explained in Section 2.4.

2.2 Quadcopter parts and components

The basic components of a quadcopter are frame, rotor blades, motors, landing gear and electronics. The frame includes the four arms onto which the rotor and motor are mounted on each, and a centre body that houses most of the electronics. The electronics used in a quadcopter include flight controller,

antenna for radio transmission, transmitter, battery and where applicable, a camera and gimbal for video and picture capturing. The battery is used to power the electronic components of the quadcopter, the gimbal is mainly used to stabilise the camera payload and the flight controller calculates the desired speeds for each rotor.

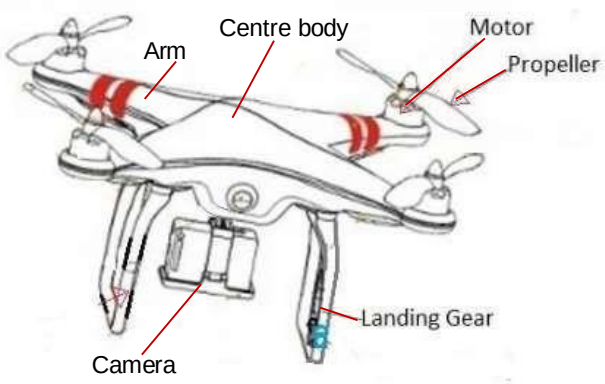

Figure 3 Basic quadcopter parts.

2.3 Quadcopter configuration

Quadcopter configuration refers to the arrangement of the four arms on a quadcopter. Quadcopter arms can be assembled in any length and arranged accordingly to suit the desired performance outcome. When designing or choosing the configuration, an engineer must consider the weight of the motors and rotors and the size of the rotors. The arms must be long enough to accommodate the length of the rotor blades so that they do not interfere with each other. Commonly used configurations include True X, Hybrid X and H shape, these can be seen in Figure 4 in Section 3.

Quadcopter configuration plays a major role in the aerodynamic performance and the ability to fly at minimal drag. This will be investigated in this project using CFD software.

2.4 Principle of operation [4]

Quadcopters are operated and controlled by varying the speed and direction at which the motors and rotor blades rotate. Two diagonally opposite rotors rotate clockwise while the other two rotate anticlockwise as shown in Figure A-1 in Appendix A. Motions such as hover, yaw, pitch and roll are achieved by adjusting the thrust produced by the rotors.

1. Hover is achieved by applying equal thrust to all four rotors.
2. Yaw is achieved by applying more thrust to two rotors rotating in one direction.
3. Pitch is achieved by applying more thrust to either the front rotors for forward pitch or back rotors for backward pitch.
4. Roll is achieved by applying more thrust to either the left-hand-side rotors for a right roll or the right-hand-side rotors for a left roll.

Figure A-1 in Appendix A, shows a photo visualization of how the above motions are achieved.

2.5 Aerodynamic forces

As a quadcopter flies through air, it experiences four major forces acting on it; drag, thrust, atmospheric pressure and weight.

1. Thrust is the force that propels the drone through air.
2. Weight is the downward force exerted on the quadcopter due to gravity. This includes weight of all components on the quadcopter.
3. Atmospheric pressure exerts a constant downward force on the quadcopter. In this project, the standard atmospheric conditions were assumed, and the pressure exerted on the quadcopter was assumed to be 101,325Pa.
4. Drag is the force that opposes the motion of the quadcopter as it flies. Drag is affected by physical quantities like area, velocity and density.

2.6 CFD

Computational Fluid Dynamics (CFD) is a numerical method of simulating steady and unsteady fluid motion using computational methods and hardware [5]. It is often used to supplement experimental and analytical methods used to analyse designs and products. CFD is less expensive to run and faster to complete compared to experimental and analytical methods such as wind tunnel testing that would require physical models to be made.

CFD uses fundamental laws of mechanics, modelling and fluid dynamics governing equations to mathematically formulate a physical problem. CFD software use numerical methods to solve the formulated problem to obtain approximate solutions for the physical properties involved [6]. CFD uses Navier-Stokes equations to solve for temperature, pressure, velocity, and density of a moving fluid. These equations are explained further in Section 2.6.1.

Factors that affect the accuracy of CFD simulations include model fidelity, mathematical models used to describe fluid behaviour, accuracy of the boundary conditions applied, resolution of the computational mesh, accuracy of the turbulence models, assumptions made and available computing resources.

Based on the resources available and allocated to this project, the CFD software chosen to conduct the simulations was Star CCM+. Star CCM+ provides a better-connected simulation process, from CAD to results, that leads easier model preparations and less computation time.

2.6.1 CFD Governing Equations [6]

There are three basic laws that govern how CFD works. These are as follows:

1. Conservation of mass equation – Continuity equation

$$\frac{\partial \rho}{\partial t} + \frac{\partial}{\partial x}(\rho u) + \frac{\partial}{\partial y}(\rho v) + \frac{\partial}{\partial z}(\rho w) = 0$$

Equation 1 – Conservation of Mass

For an incompressible flow, the density of the fluid is constant, and the equation is reduced to

$$\frac{\partial}{\partial x}(u) + \frac{\partial}{\partial y}(v) + \frac{\partial}{\partial z}(w) = 0$$

Equation 2 – Simplified Conservation of Mass

2. Conservation of momentum – Navier Stokes equation.

$$\frac{\partial \vec{v}}{\partial t} + \vec{v} \cdot \nabla \vec{v} = \vec{f} - \nabla p + \mu \nabla^2 \vec{v}$$

Equation 3 – Conservation of Momentum

Where the first term represents local change with time, the second term represents momentum convection, the third term represents mass force, the fourth term represents surface force, and the fifth term represents the diffusion term.

3. Conservation of energy – Newton's First Law of Thermodynamics

$$\rho \left(\frac{\partial e}{\partial t} + u \frac{\partial e}{\partial x} \right) = -p \left(\frac{\partial u}{\partial x} + \frac{\partial v}{\partial y} + \frac{\partial w}{\partial z} \right) + \frac{\partial}{\partial x}\left(k \frac{\partial T}{\partial x} \right) + \Phi$$

Equation 4 – Conservation of Energy

Where the first term represents local change with time, the second term represents momentum convection, the third term represents surface force, the fourth term represents the diffusion term, and the fifth term represents mass force.

CFD software solves the above-mentioned governing equations iteratively to arrive at the simulation results. A steady-state flow simulation with a uniform or fabricated flow field and iterating over time until the steady-state flow field is obtained.

2.6.2 Turbulence Models [7],[8]

These are methods in CFD used to include the effect of turbulence in the simulation of fluid flows. CFD mathematically simulates and estimates how turbulent flow behaves in a flow as they are characterised with irregular fluctuations in the pressure and velocity of the fluid.

The following are commonly applied turbulent models in CFD analysis:

1. Spalart-Allmaras. This model uses one equation that solves for the Turbulent Eddy Viscosity. It provides accurate predictions for incompressible flows, but it is not suitable for flows with complex geometries.
2. K-epsilon. This model uses two equations to solve for turbulent kinetic energy and its dissipation rate. It has good accuracy for both compressible and incompressible flows, but it lacks accuracy for non-slip walls. Usually used in flows with high Reynolds number or freestreams.
3. K-omega. This model uses two equations to solve for turbulent kinetic energy and the specific dissipation rate of turbulence (omega). This model accurately predicts flow near the boundaries and provides better accuracy for complex flows compared to the k-epsilon model.

The turbulence model chosen to conduct the CFD simulations in this project was k-omega.

3. CAD Modelling

Four quadcopters with four different arm configurations were designed on CATIA v5. The configurations were True X, H, Plus and Hybrid X. To ensure that the models are analogous, the middle parts of each quadcopter model had the same dimensions, and the rotors were positioned 400mm from each other except for the Hybrid X model. These dimensions were chosen based on commonly used quadcopters that already exist.

Each model is made up of 4 basic parts; top body part, bottom body part, landing gears positioned under the rotor and a middle layer with the arms. Due to the nature at which the CFD simulations were conducted on the quadcopters, thrust was not required and therefore there was no need for the rotor blades and motors to be included in the design models instead circular parts at the end of each arm were added to represent where the motors and rotors were to be positioned. Engineering drawings of each model outlining the key components and dimensions can be found in Appendix B.

The quadcopter models were made in collaboration with Beatriz da Mata Ribeiro as the models need to be analogous to provide a more accurate comparison.

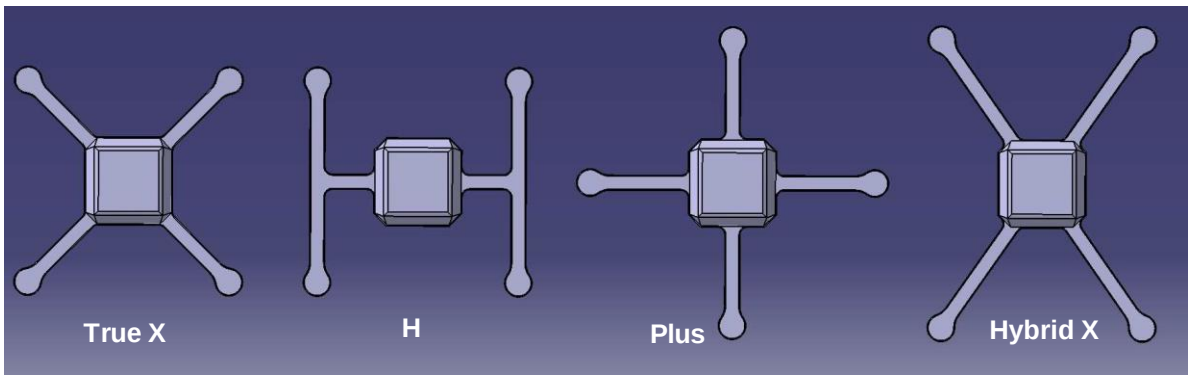

Figure 4 - A photo of all four quadcopter models side-by-side on CATIA v5.

3.1 True X Model

This model was designed to resemble the shape of the letter X with each arm positioned 90º from each other. The first arm is positioned 45º from the horizontal axis as shown in the sketch below. Each rotor is positioned 400mm from each other. A detailed sketch of the model can be found in Figure B-1 in Appendix B.

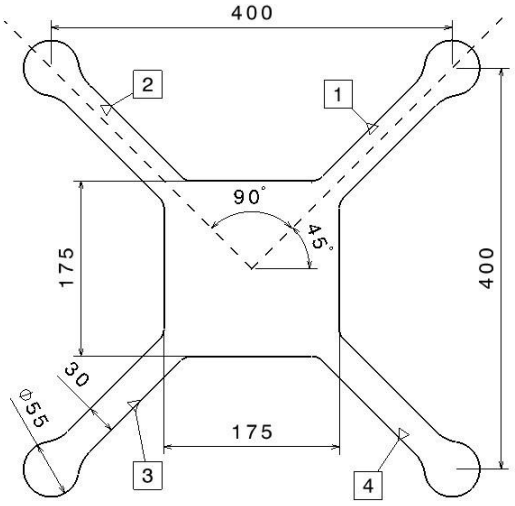

Figure 5 - A basic sketch of the arms on true X model on CATIA v5.

3.2 H Model

This model was designed to resemble the shape of the letter H. The model has two arms emerging from the centre body that branch out into two more arms, making a total of four arms. The two arms that emerge from the centre body are positioned 180° from each other as shown in the sketch below. The rotors on this model were also positioned 400 mm from each other. A detailed sketch of the model can be found in Figure B-2 in Appendix B.

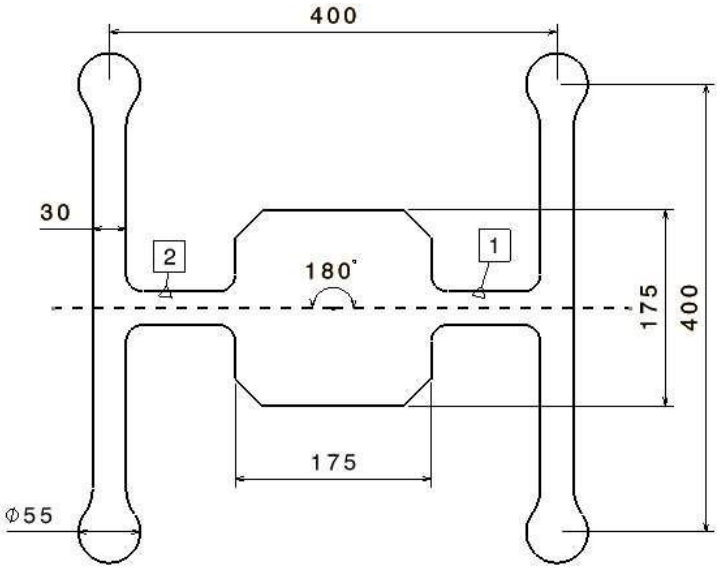

Figure 6 - A basic sketch of the arms on H model on CATIA v5.

3.3 Plus Model

This model was designed to resemble the '+' symbol. Each arm is positioned 90º from each other with the first arm positioned 90º from the horizontal axis. Each rotor was positioned 400 mm from each other. A detailed sketch of the model can be found in Figure B-3 in Appendix B.

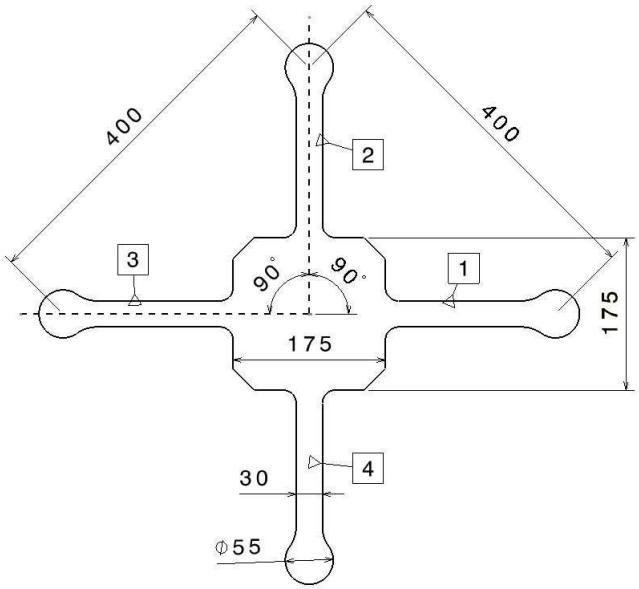

Figure 7 - A basic sketch of the arms on plus model on CATIA v5.

3.4 Hybrid X Model

This model was designed to resemble the letter X, however, in order to elongate the arms, the angle between the arms was varied. The first arm was positioned 55° from the horizontal axis, the second arm was positioned 70° from the first arm. The third arm was positioned 110° from the second arm and the fourth arm was positioned 70° from the third arm. Due to the angles used to create the models, it was not possible to maintain the 400mm spacing among all four rotors. The first and second rotors have a 400mm spacing between each other and the third and fourth rotors also have a 400mm spacing from each other. A detailed sketch of the model can be found in Figure B-4 in Appendix B.

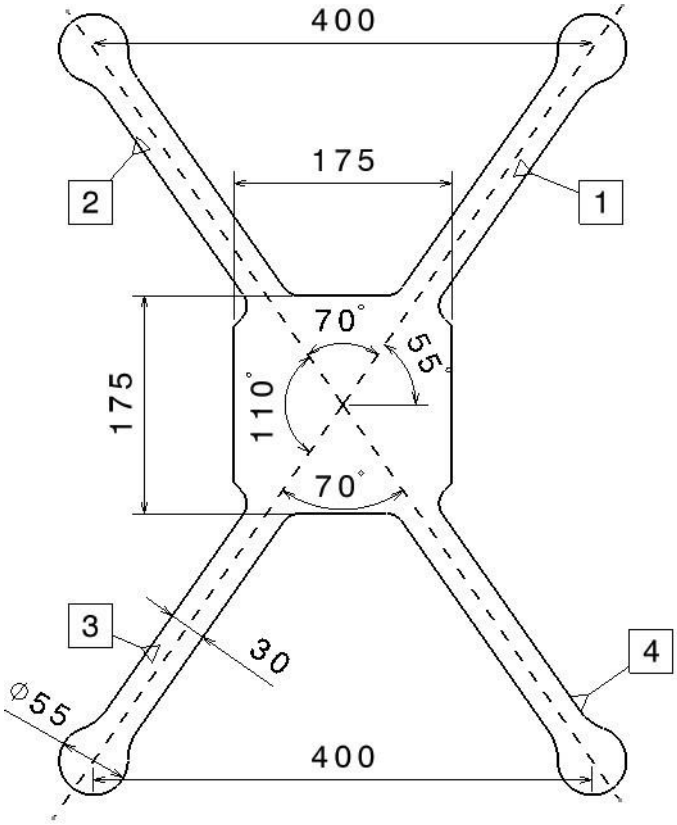

Figure 8 - A basic sketch of the Hybrid X model on CATIA v5.

4. CFD Methodology

To analyse the aerodynamic behaviour of the quadcopter models under different velocities, CFD simulations were run using the Star CCM+ software. To simulate the motion of a quadcopter as it flies in air, airflow was made to pass through the quadcopter models at different velocities. The velocities that were simulated were 40, 30, 20, 10, 5, 4, 3, 2 and 1mph. Typically, the cruise velocities of a quadcopter ranges between 20mph to 40mph which were simulated in the project and lower velocities were simulated as well, in order to analyse quadcopter performance at low velocities.
This section outlines the process that was used to conduct the CFD simulation from pre-processing to post processing. These steps were applied in all simulations of the four quadcopter models and the validation models.

4.1 Pre-processing

1. The CAD model was imported to Star CCM+. Since the model was an assembly design, a Boolean unite operation was used to join all the body parts into one body.
2. From the CAD model, a new geometry part was generated.
3. A boundary block covering only half the model was created. This was done to reduce the time taken for Star CCM+ to solve the simulation. The boundary block had the corner coordinates: (-1.5, 0, -0.5) m and (1.5, 1, 0.5) m. Figure A-2 in Appendix A shows an example of the boundary block made for the True X model.
4. The boundary block was split by patch and the surfaces were renamed accordingly. These surfaces are inlet, outlet, slip walls and symmetry plane.
    - The surface that was directly opposite to the front face of the quadcopter was the inlet.
    - The surface that was directly opposite to the back side of the quadcopter was the outlet.
    - The surface that passed through the middle of the quadcopter was the symmetry plane.
    - The remaining three surfaces were the slip walls.

    Figures A-3 and A-4 in Appendix A shows an example of the surfaces mentioned above as seen on the True X model.
5. A Boolean subtract was created from the boundary block and the geometry part.
6. Parts were assigned to the subtract, creating a boundary layer for each part surface. Table 1 shows the boundaries assigned to the regions. This was done to identify the inlet surface where the flow came in and the outlet where the flow went out. It also ensured that prism layers formed around the quadcopter model only and not the boundary block during meshing.

Region	Boundary type
Inlet surface	Velocity inlet
Outlet surface	Pressure outlet
Symmetry wall	Symmetry plane
Slip walls	Wall
Quadcopter geometry	Wall

Table 1 - Boundary type assigned to each region.

7. A small block was created and the snap to part function was applied. This block was used to create the fine mesh on the quadcopter model.
8. An automated mesh was created and the following meshers used were Surface Remesher, Automatic Surface Repair, Trimmed Cell Mesher and Prism Layer Mesher.
9. The default controls used for the simulation were as follows:

Name of Mesh Setting	Value/ Setting used
Base size	0.5 - 0.2
Number of Prism layers	4
Prism layer stretching	1.2
Prism layer total thickness	1%
Volume default growth rate	Very slow
Surface growth rate	Very slow
Maximum cell size	5000

Table 2 - Default mesh controls used for the CFD simulations.

All other controls such as surface curvature, surface proximity and CAD projection were kept at default settings.

10. The volumetric controls used were surface remesher and a customized isotropic size of 1.
11. After the meshing was executed, section planes were used to visualize the mesh cells formed. Figures A-6 to A-10 in Appendix A show the mesh visualization for all four quadcopter models.
12. Thereafter, the physics models were chosen and applied. The physics models used are explained further in Section 4.3.
13. The initial velocity conditions for the physics model were put in with reference to the position of the inlet surface.
14. The velocity for the inlet surface was also changed to match the velocity used in the initial conditions of the physics model.
15. Two force reports were generated, one for downforce and another for drag. The reference pressure used was 101,325Pa for both reports. The drag force acted in a direction opposing the motion of the quadcopter while the downforce acted downwards on the model. For example, in Figure 9 the drag force acted in the -x axis direction while the downforce acted in the -z axis direction.

Figure 9 - Boundary block with reference axes.

16. After the reports are created, a single plot and monitor was made for both reports. The single plot displayed the values of drag and downforce for each iteration.
17. Thereafter, the simulations were run until they achieved an acceptable number of iterations which was determined by the drag plot. Once the value for drag converged to a steady state value where there were no significant changes for at least 100 iterations, the simulation was stopped.

4.2 Post-processing

Once the simulations were done running, the values for drag were exported from Star CCM+ to Excel for analysis. Additionally, a vector scene showing airflow around the quadcopter models and a scalar scene showing pressure on the models and streamlines were both generated for each simulation. These have been discussed further in Section 6.

4.3 Physics continuum [9]

These are the physics models and solution methods used to run and solve the simulations. The physics models used to in the simulations were as follows:

Physical Property	Chosen Model
Spatial dimensions	Three dimensional
Time	Steady
Material	Gas
Flow	Segregated flow
Equation of state	Constant density
Viscous regime	Turbulent
Turbulence model	K-omega Turbulence
Optional model	Cell quality remediation

Table 3 Physics models chosen for the simulations.

By selecting the above physics models, the solution methods that were automatically chosen by the software were All y+ Wall Treatment, Exact Wall Distance, SST (Menter) K-Omega, Reynolds-Averaged Navier Stokes and Gradients.

For the gas model, the density and dynamic viscosity of air were used. The value of density was 1.1845kg/m^3 and dynamic viscosity was 1.85508 e^{-5}Pa•s. In addition to this, the atmospheric pressure exerted on the quadcopter was assumed to be 101,325Pa.

4.4 Mesh analysis and convergence

The process of mesh convergence is the process of decreasing the mesh size and analysing the impact it has on the accuracy of the solution. Typically, the smaller the mesh size, the more accurate the solution as the behaviour of the model is better sampled across its physical domain[19]. A finer mesh can capture more detail and reduce numerical errors, but it increases computational cost and time.

For this project, the mesh convergence process was done using mesh visualisation and comparison of the drag results of the simulations for each mesh setting. The mesh default controls that were varied

during this process were: core volume mesher, base size, number of prism layers, prism layer thickness and volume growth rates. All other meshing controls were either changed to a constant setting or used the preset settings automatically chosen by the software.

The first mesh controls were used to produce a coarse mesh, then the controls were reduced to refine the mesh and produce a finer mesh on the model.

As the four quadcopter models were analogous, only one model was used for the mesh analysis to establish the appropriate mesh size.

4.4.1 Core volume mesher [10]

The two types of meshers that were investigated were trimmed cell mesher and polyhedral volume mesher.

1. Trimmed cell mesher creates hexahedral cells in a grid across the entire region that is being meshed. It is mostly used in external aerodynamic cases.
2. Polyhedral volume mesher builds tetrahedrons that are then combined to generate a poly mesh with a lower number of cells. It is usually used in internal flows.

Between the two core volume meshers mentioned above, only the trimmed cell mesher was successful as the polyhedral volume mesher took hours to mesh and produced inconsistent results. Hence, the trimmed cell mesher was the chosen mesh setting.

4.4.2 Prism Layers

These are prism shaped cells that project the mesh faces from the core mesh onto the solid boundary [11]. These cells form a layer or layers around the surface of the model to capture boundary effects like friction and flow separation. Two parameters were varied to determine the appropriate prism layer controls: number of prism layers and prism layer thickness. These parameters were varied until thin rectangular shaped prism layers cells formed flat around the quadcopter model.

When the number of prism layers was set to 2, the prism layers did not produce the desired shape, however when it was increased to 3 the desired shape was achieved but the prism layers did not form well on corners and rounded surfaces. The numbered was then increased to 4 which gave the desired shape for the prism layer and formed well around the whole quadcopter model.

A similar pattern was observed when varying the prism layer thickness. When the prism layer thickness was set to 33% of the base size, the prism layers generated did not have the desired shape and did not form well around the quadcopter as seen in Figure A-6 in Appendix A. However, as the thickness was reduced to 2.5% and 1% of the base size, the prism layer cells with the desired shape formed properly around the surface of the quadcopter as seen in Figures A-9 and A-10 in Appendix A.

4.4.3 Base size

This is the starting cell size used to set other mesh parameters like prism layer thickness and target size [12]. The base sizes that were analysed were 0.5m, 0.4m, 0.3m and 0.2m.

- At 0.5m base size, the mesh was coarse, and the prism layers did not fully form around the quadcopter model. This can be seen in Figures A-6 and A-7 in Appendix A.
- At 0.4m base size, the mesh was still coarse, and the prism layers were not generated properly around the model especially on the corners and rounded edges as seen in Figures A-8 in Appendix A.
- At 0.3m and 0.2m base size, the mesh was more refined, and the prism layers were formed properly around the surface of the quadcopter. Figures A-9 and A-10 in Appendix A shows the mesh visualisation of the two base sizes, from the figures the significant difference between the two base sizes is that there are more mesh cells concentrated around the quadcopter model in the 0.2m base size than in the 0.3m base size.

Other than the mesh visualisation, the models were simulated to compare the drag results produced with each base size. There was significant change as the base size was reduced from 0.5m to 0.3m. However, there was insignificant change between the drag values obtained at 0.3m and 0.2m base sizes. Figure 10 shows a plot of drag against base size at 10mph, the same trend was observed at other velocities. It was then established the appropriate mesh base sizes were 0.3m and 0.2m.

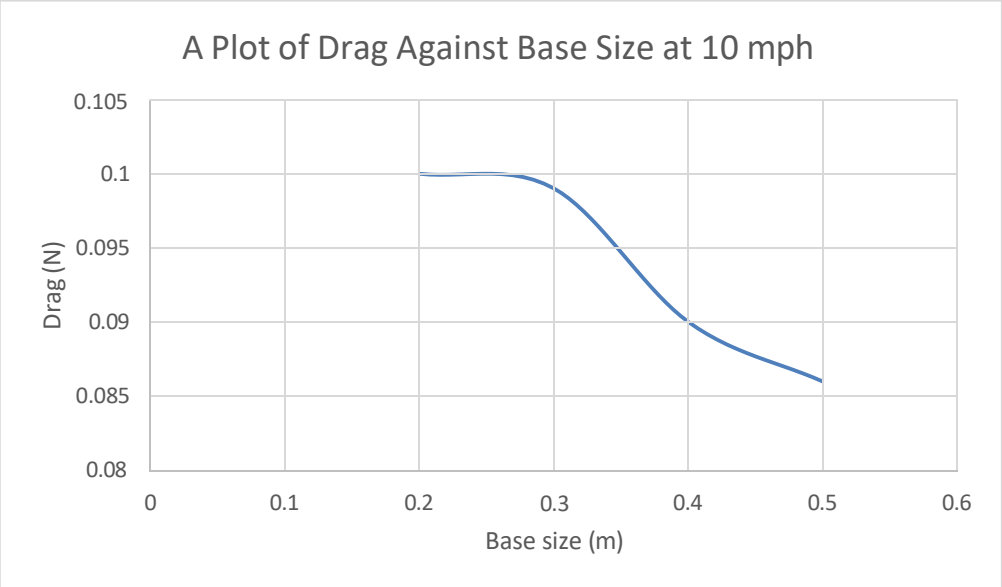

Figure 10 A plot of Drag against base size at 10mph.

4.4.4 Final Mesh controls

Based on the accuracy effects of the mesh controls discussed above, the mesh controls outlined below were the ones used to carry out the simulations:

1. Base size = 0.3m
2. Number of prism layers = 4
3. Prism layer stretching = 1.2
4. Prism layer thickness = 1%
5. Volume growth rate = very slow
6. Maximum cell size = 5000

5. Validation

In order to validate the methodology chosen to conduct the CFD simulation of the quadcopters, CFD simulations were run on two blunt bodies using the same methodology outlined above to find their coefficients of drag. One of the blunt bodies that was simulated was a flat plate and the other was a bullet. Equation 5 was used to calculate the coefficient of drag from the extracted drag value.

$$C_d = \frac{D}{\frac{1}{2}\rho v^2 S}$$

Equation 5 – Drag Equation [20]

Where C_d = drag coefficient, D = drag, ρ = density of air, v = velocity at which the quadcopter is moving and S = effective frontal area.

The drag coefficients obtained from the CFD simulations were compared to the pre-established C_d values for the blunt bodies. A 5% margin was applied as the acceptance criteria for the calculated C_d values.

5.1 Flat plate

Figure 11 shows the drag plot for the flat plate, the value of drag settles at a steady state value of 0.629007N.

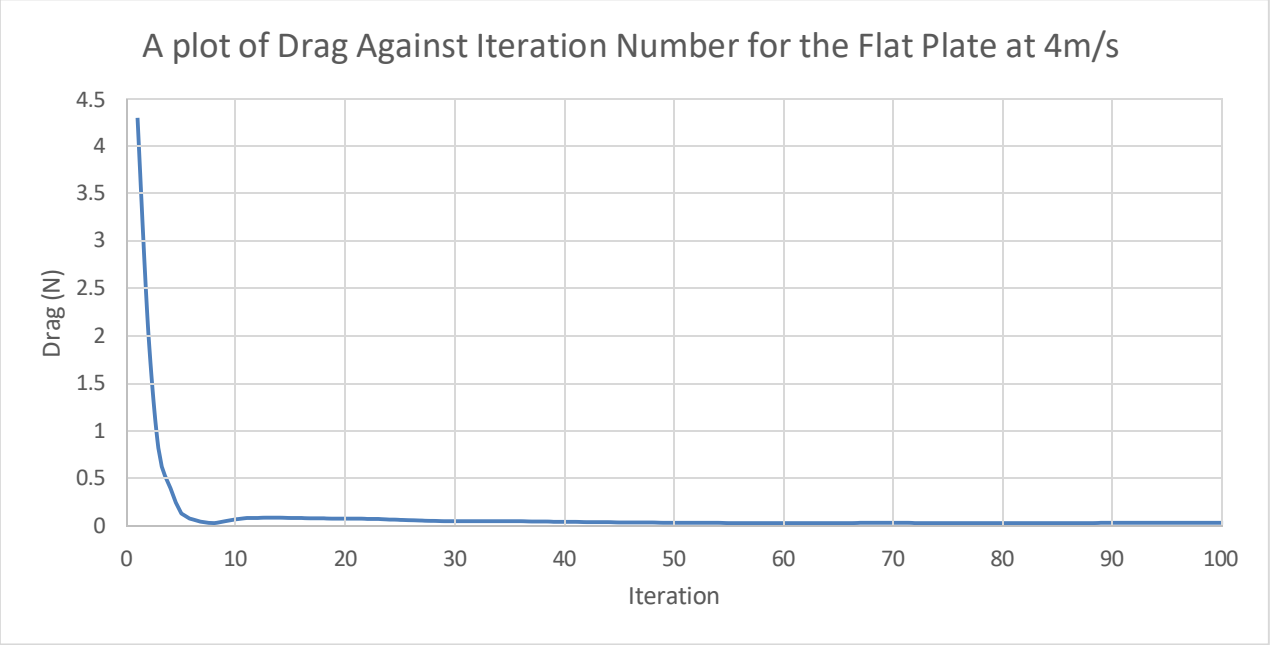

Figure 11 Drag plot for the flat plate simulated at 4m/s.

Using Equation 1 and the parameters in Table 4, the calculated coefficient of drag was 1.253. This value is within the 5% margin of the pre-established C_d value for a flat plate which is 1.28 [13].

Flat plate parameters	
D	0.629007N
ρ	1.18415kg/m^3

v	4 m/s
S	0.0265 m^2

Table 4 Flat plate parameters.

Figure 12 shows the pressure distribution and velocity flow field around the bullet as it moves through air at 4m/s. Figure A-11 in Appendix A shows a detailed picture of the pressure distribution on the flat plate. From this figure it can be seen that the front face, especially the centre, of the flat plate experienced higher pressure compared to the back side of the flat plate. The back face of the model experienced the lowest pressure as seen Figure A-12 in Appendix A.

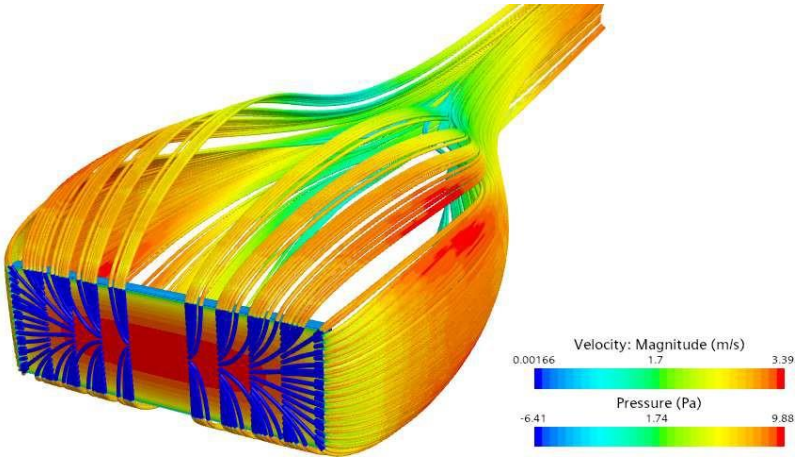

Figure 12 Pressure distribution and velocity profile of the flat plate.

Figure 13 shows the airflow in the boundary layer surrounding the bullet model.

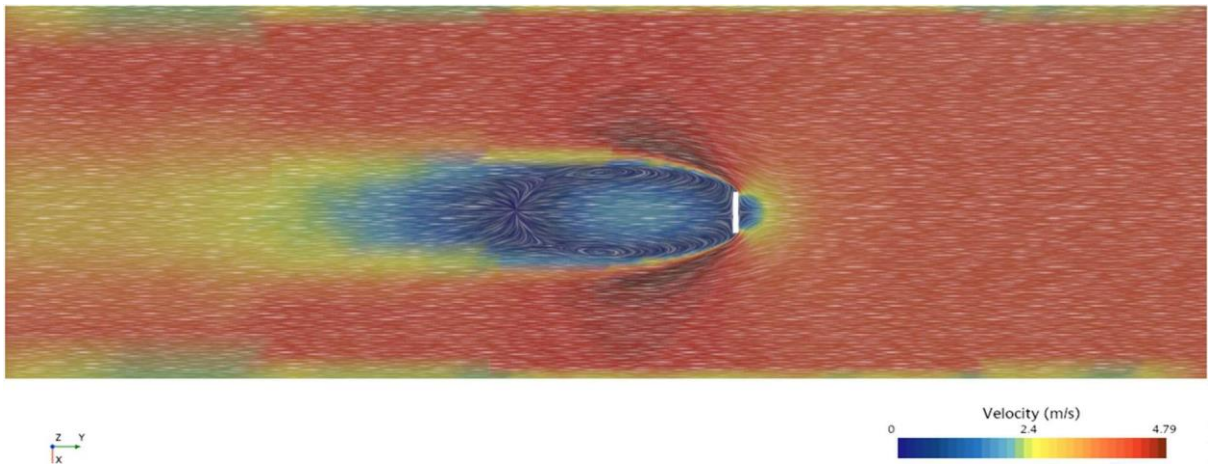

Figure 13 Airflow surrounding the flat plate model at 4m/s.

5.2 Bullet

Figure 14 shows the drag plot for the bullet, the value of drag settles at a steady state value of 0.056562N.

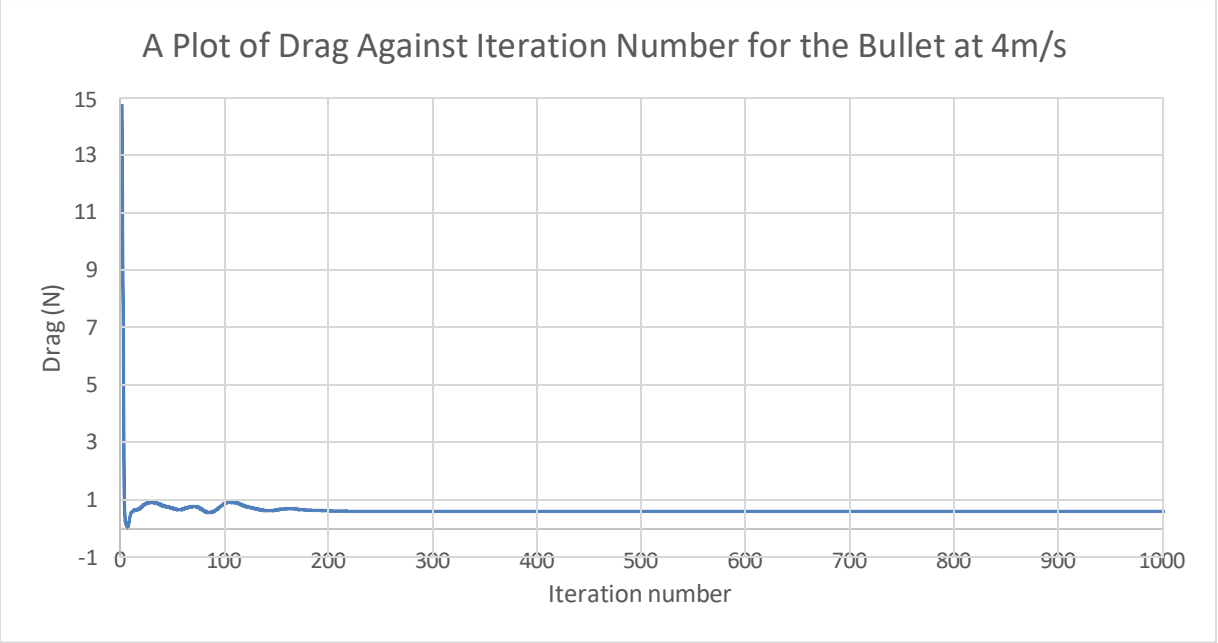

Figure 14 Drag plot for the bullet simulated at 4m/s.

Using equation 1 and the parameters in Table 5, the calculated coefficient of drag was 0.2983. This value is within 5% margin of the pre-established C_d value for a flat plate which is 0.295 [13].

Bullet parameters	
D	0.05652 N
ρ	1.18415 kg/m^3
v	4 m/s
S	0.02 m^2

Table 5 Bullet parameters.

Figure 15 shows the pressure and velocity flow field around the bullet as it moves through air at 4m/s. Figure A-13 in Appendix A shows a detailed picture of the pressure distribution on the bullet. From this figure it can be seen that the tip of the bullet experiences the highest pressure compared to other parts of the model.

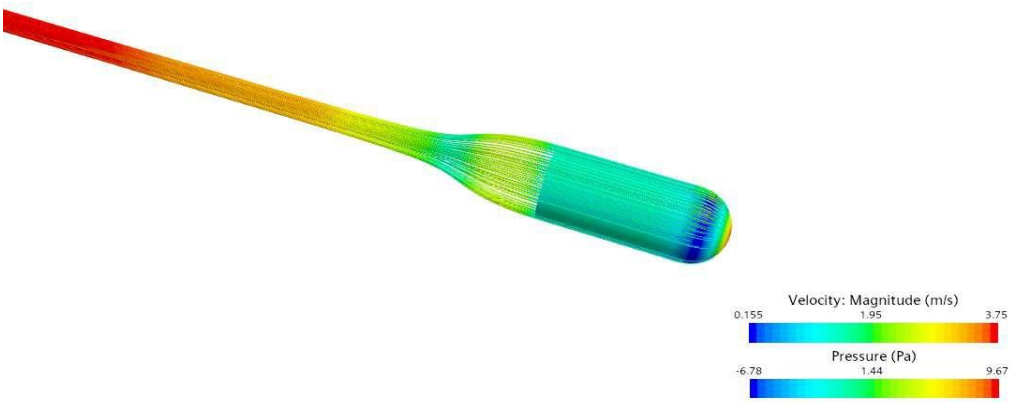

Figure 15 Pressure and velocity fields of the bullet at 4m/s.

Figure 16 shows the airflow in the boundary layer surrounding the bullet model.

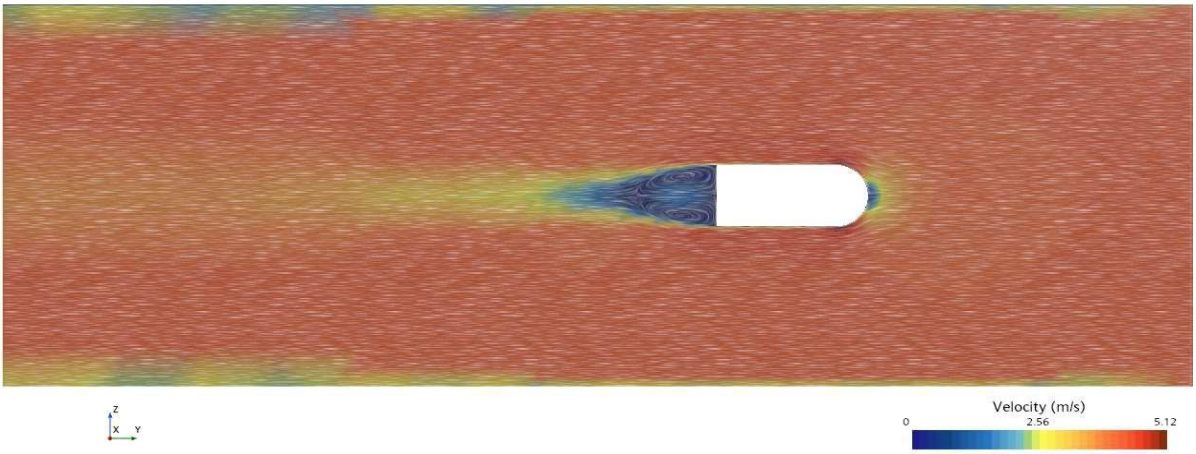

Figure 16 Airflow surrounding the bullet model at 4m/s.

6. Results

From the simulations, the values of drag were extracted and analysed on excel. From the drag values, the coefficient of drag (C_d) was calculated using Equation 6.

$$C_d = \frac{D}{\rho * v^2 * S}$$

Equation 6 – Drag Equation [20]

Where D = drag, ρ = density of air, v = velocity at which the quadcopter is moving and S = quadcopter frontal cross-sectional area (effective area).

Table 6 shows the estimated cross-sectional area of the models.

Model	Area (m^2)
True X	0.028
H	0.034
Plus	0.333
Hybrid X	0.03

Table 6 Estimated cross-sectional area of the quadcopter models.

6.1 True X Model Results

The True X model had the second highest overall values of drag. Based on the result in Table 7, it was observed that drag increased with an increase in velocity.

Velocity (mph)	40	30	20	10	5	4	3	2	1
Drag (N)	2.65	1.5099	0.6902	0.1985	0.0575	0.0379	0.0219	0.0114	0.0027

Table 7 Drag values for the True X model at different velocities.

From the above values, the value of C_d calculated using Equation 6 was 0.53165.

This increase was not linear, rather it was exponential as seen in the drag plot in Figure 17.

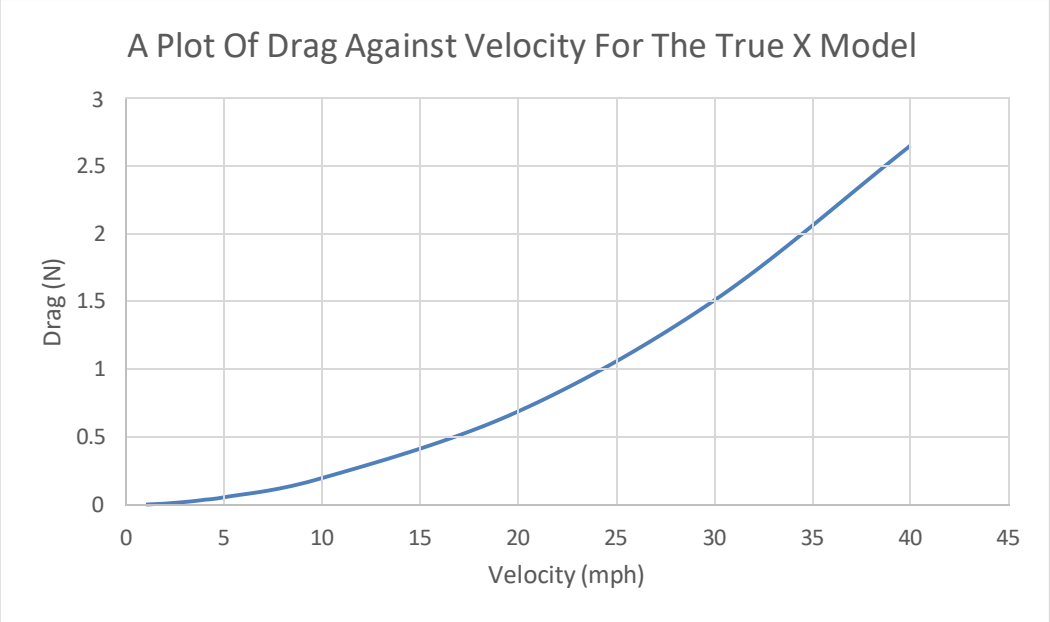

Figure 17 Drag plot for the True X model at varying velocities.

Figure 18 shows an example of the pressure distribution and velocity fields of the True X model at 10mph. Figures A-14, A-15 and A-16 in Appendix A show more pressure distribution and velocity fields of the True X model at varying velocities. By analysing these figures, it is evident that the frontal area (including the centre body, arms and landing gear) of the quadcopter experienced higher pressure than the rest of the quadcopter.

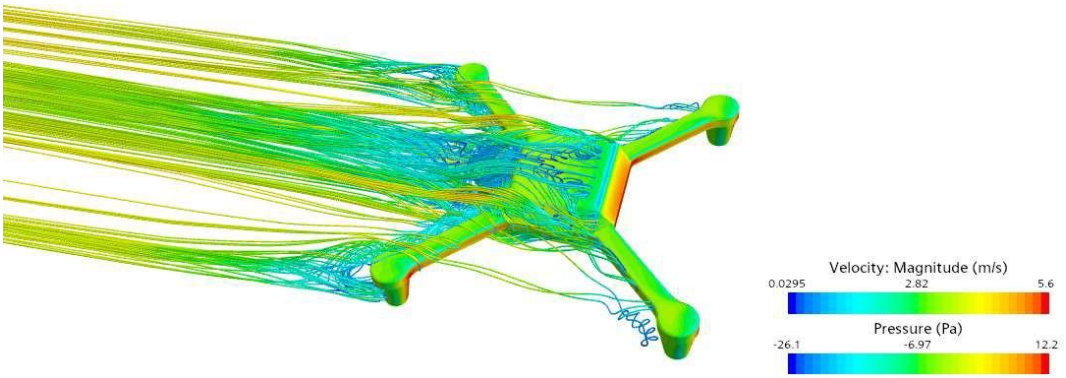

Figure 18 Pressure distribution and velocity fields of the True X model at 10mph.

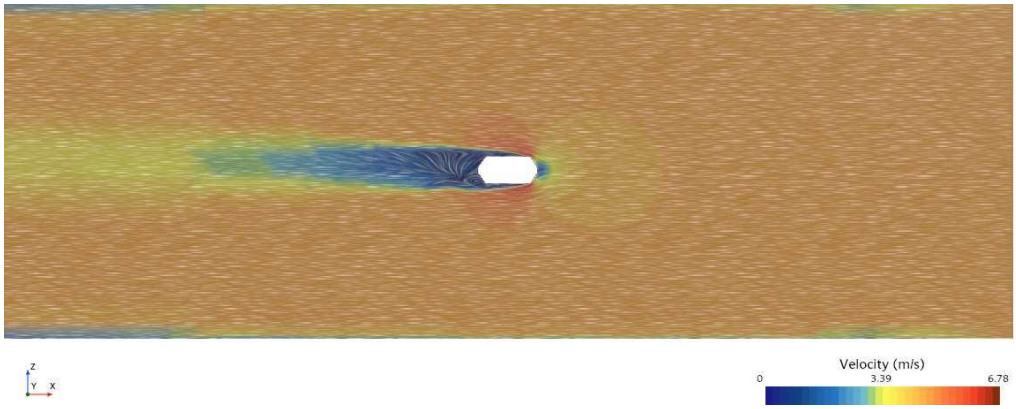

Figure 19 Velocity contours around the True X model showing the airflow around it at 10mph.

6.2 H model results

The True X model had the second lowest overall values of drag. Based on the result in Table 8, it can be seen that drag increased with an increase in velocity

Velocity (mph)	40	30	20	10	5	4	3	2	1
Drag (N)	2.4418	1.4071	0.6263	0.1792	0.0535	0.0025	0.0208	0.0096	0.0024

Table 8 Drag values for the H model at different velocities.

From the above values, the value of Cd calculated using Equation 6 was 0.40072.

This increase was not linear, rather it was exponential as seen in the drag plot in Figure 20.

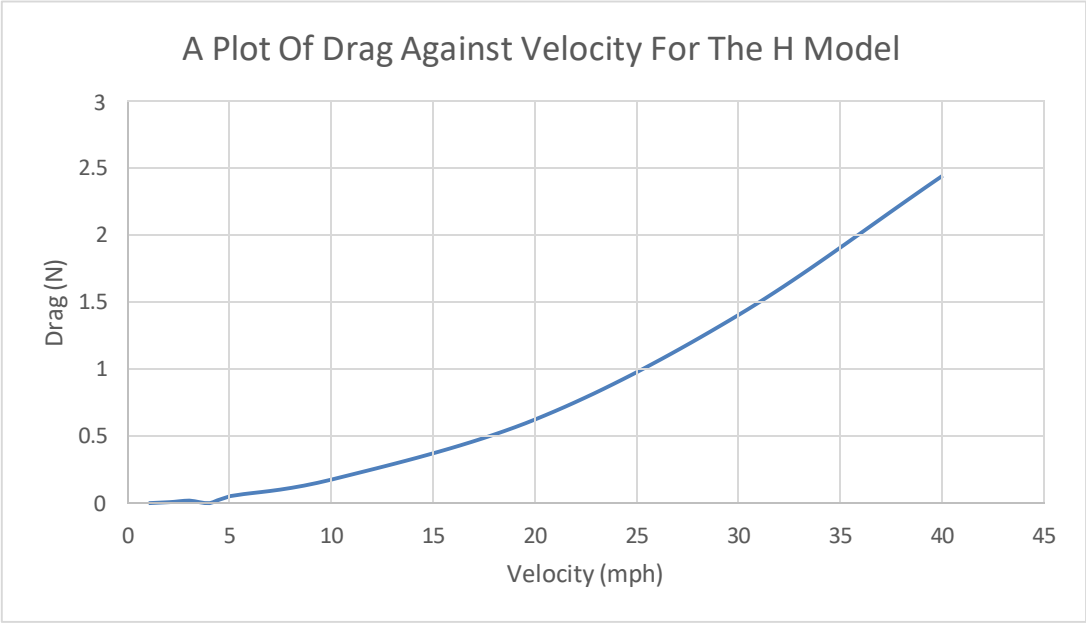

Figure 20 Drag plot for the H model at varying velocities.

Figure 21 shows an example of the pressure distribution and velocity fields of the H model at 10mph. Figure A-17 and A-18 in Appendix A show more pressure distribution and velocity fields of the True X model at varying velocities. By analysing these figures, it is evident that the frontal area (including the

centre body, arms and landing gear) of the quadcopter experienced higher pressure than the rest of the quadcopter.

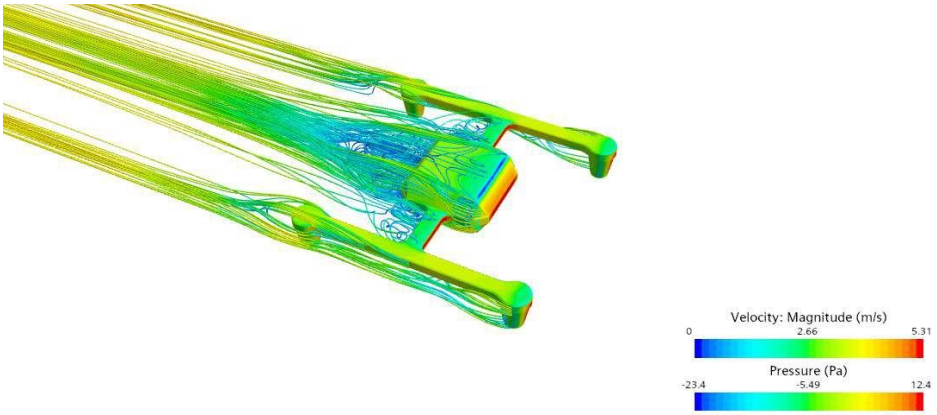

Figure 21 Pressure distribution and velocity profile of the H model at 10mph.

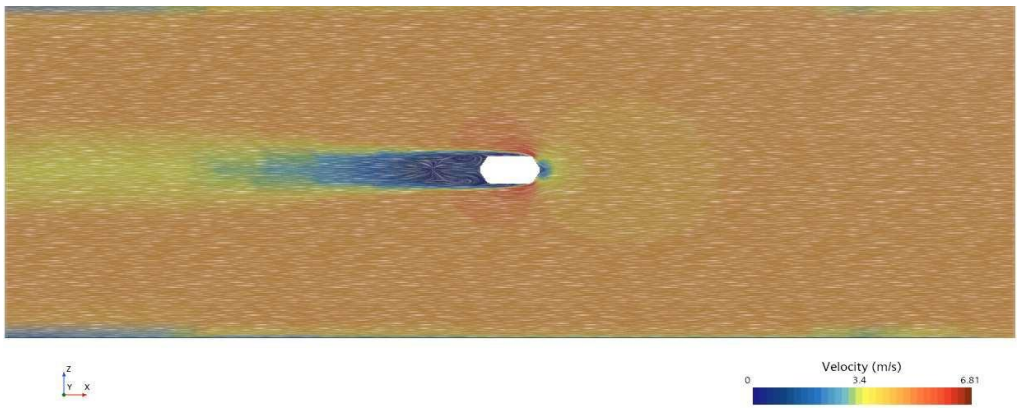

Figure 22 Velocity contours around the H model showing the airflow around it at 10mph.

6.3 Plus Model Results

The True X model had the highest overall values of drag, making the Plus configuration the least aerodynamic based on the drag values obtained. Based on the result in Table 9, it can be seen that drag increased with an increase in velocity

Velocity (mph)	40	30	20	10	5	4	3	2	1
Drag (N)	3.3001	1.886	0.8660	0.2268	0.0639	0.0416	0.0246	0.0113	0.00295

Table 9 Drag values for the Plus model at different velocities.

From the above values, the value of Cd calculated using Equation 6 was 0.54522.

This increase was not linear, rather it was exponential as seen in the drag plot in Figure 23.

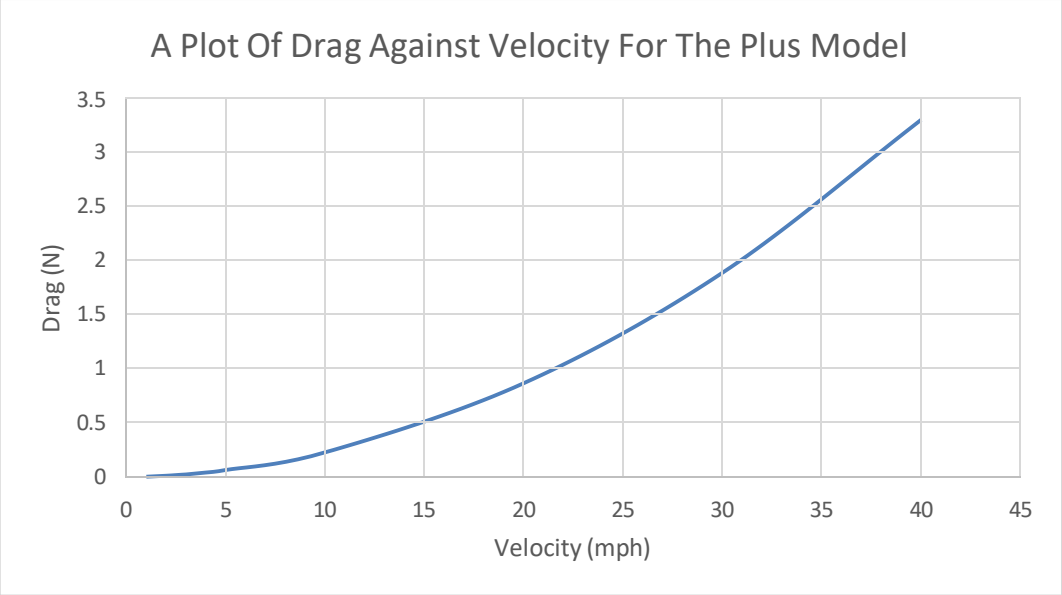

Figure 23 Drag plot for the Plus model at varying velocities.

Figure 24 shows an example of the pressure distribution and velocity fields of the Plus model at 10mph. Figures A-19 and A-20 in Appendix A show more pressure distribution and velocity fields of the True X model at varying velocities. By analysing these figures, it is evident that the frontal area (including the centre body, arms and landing gear) of the quadcopter experienced higher pressure than the rest of the quadcopter.

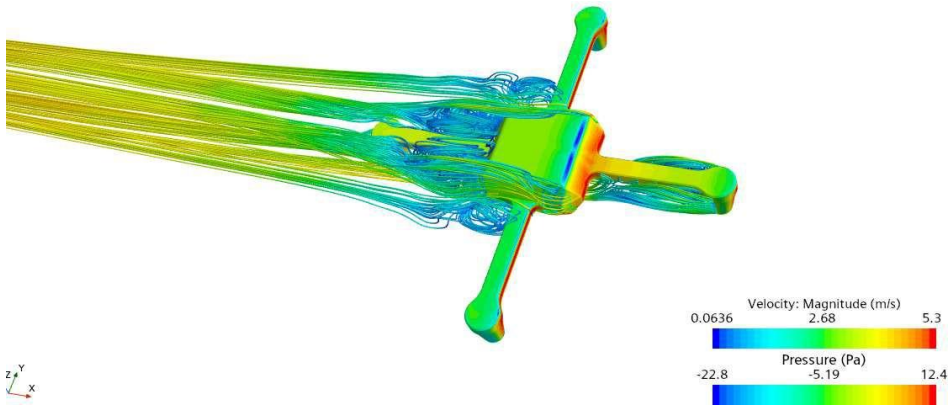

Figure 24 Pressure distribution and velocity profile of the Plus model at 10mph.

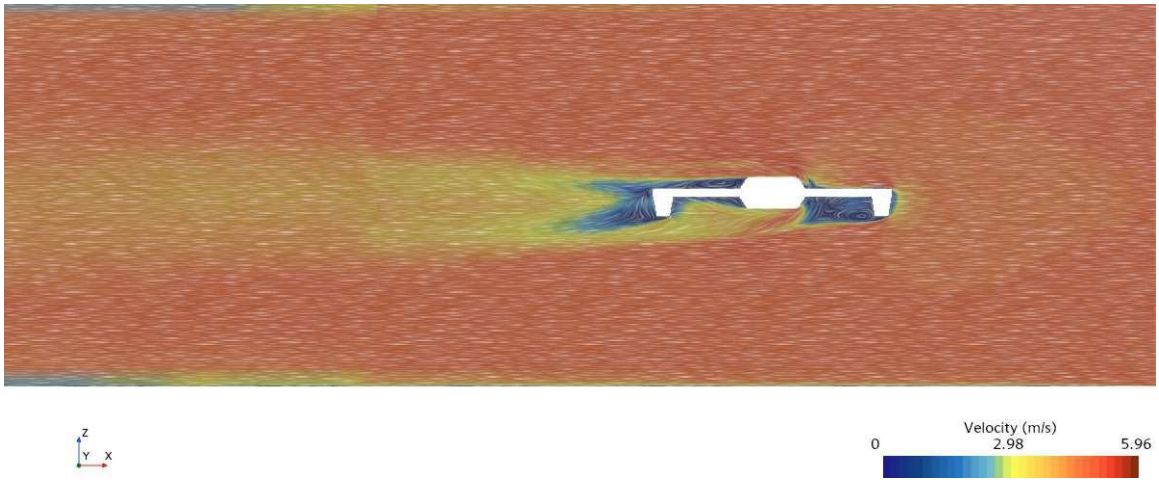

Figure 25 Velocity contours around the Plus model showing the airflow around it at 10mph.

6.4 Hybrid X Model Results

The True X model had the lowest overall values of drag, making it the most aerodynamic configuration based on drag values. Based on the result in Table 10, it can be seen that drag increased with an increase in velocity

Velocity (mph)	40	30	20	10	5	4	3	2	1
Drag (N)	2.1816	1.2322	0.5771	0.1690	0.0508	0.0336	0.0195	0.00908	0.0024

Table 10 Drag values for the Hybrid X model at different velocities.

From the above values, the value of Cd calculated using Equation 6 was 0.41319.

This increase was not linear, rather it was exponential as seen in the drag plot in Figure 26.

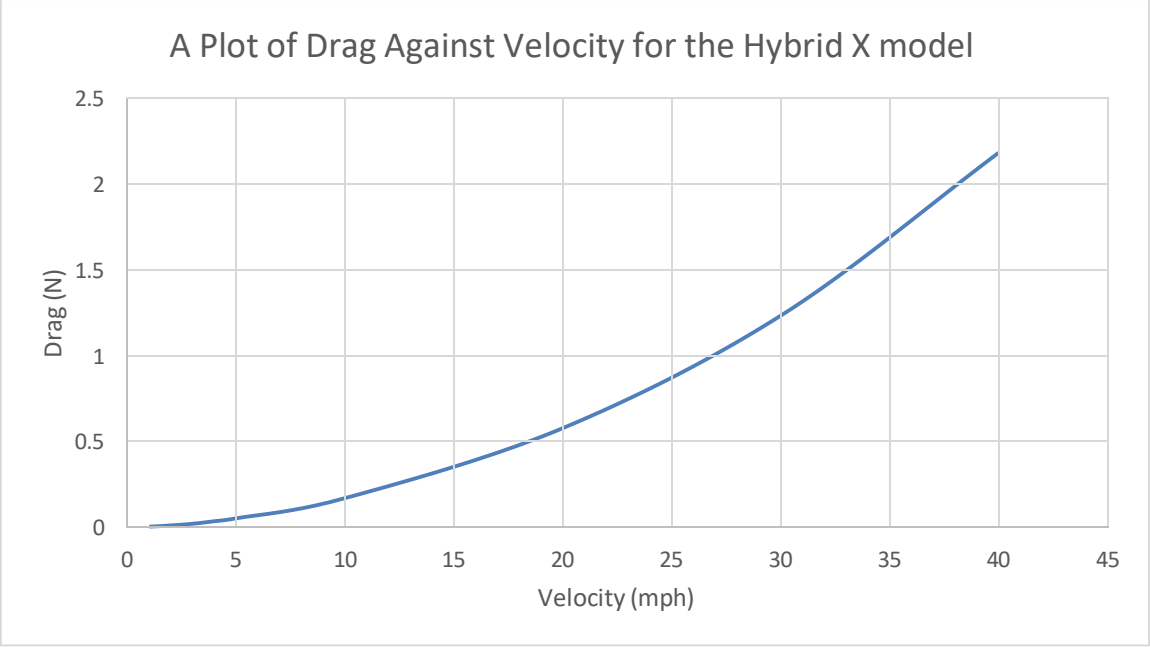

Figure 26 Drag plot for the Hybrid X model at varying velocities.

Figure 27 shows an example of the pressure distribution and velocity fields of the Plus model at 10mph. Figures A-21 and A-22 in Appendix A show more pressure distribution and velocity fields of the True X model at varying velocities.

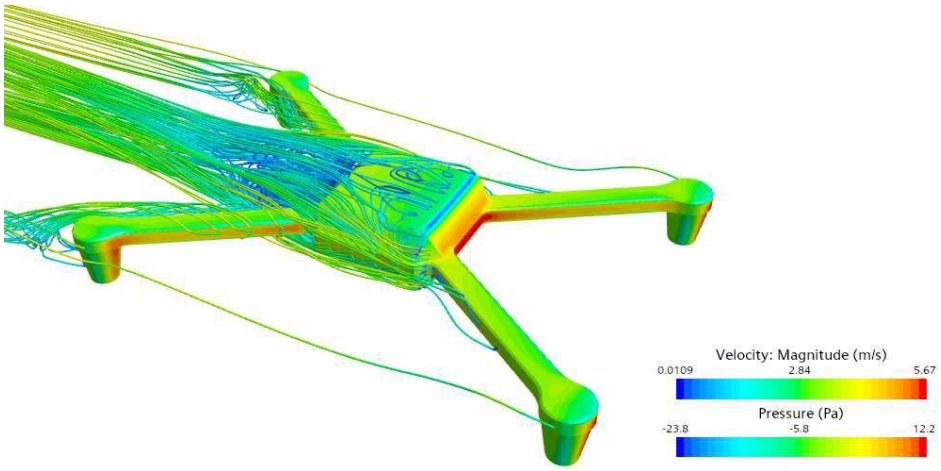

Figure 27 Pressure distribution and velocity profile of the Hybrid X model at 10mph.

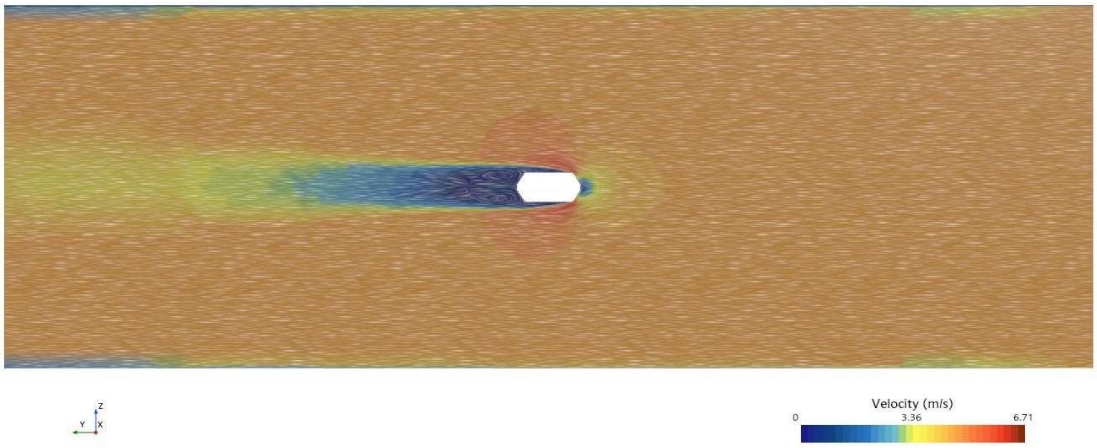

Figure 28 Velocity contours around the Hybrid X showing the airflow around it at 10mph.

6.5 Results comparison

Table 11 summarizes the values of drag for each model for each velocity. From these results, the Hybrid X model experienced the least drag out of all four models while the Plus model experienced the highest drag.

	Drag (N)			
Velocity (mph)	**True X**	**H**	**Plus**	**Hybrid X**
40	2.650004	2.441803	3.300046	2.181636
30	1.509909	1.407076	1.886026	1.232216
20	0.690237	0.626261	0.866021	0.577104
10	0.198477	0.179208	0.226834	0.169042
5	0.057465	0.053484	0.06389	0.050834
4	0.037858	0.002488	0.041612	0.033588
3	0.021865	0.020769	0.02464	0.019456
2	0.011359	0.009582	0.011289	0.009086
1	0.002707	0.002488	0.002952	0.002434

Table 11 Drag comparison of the quadcopter models.

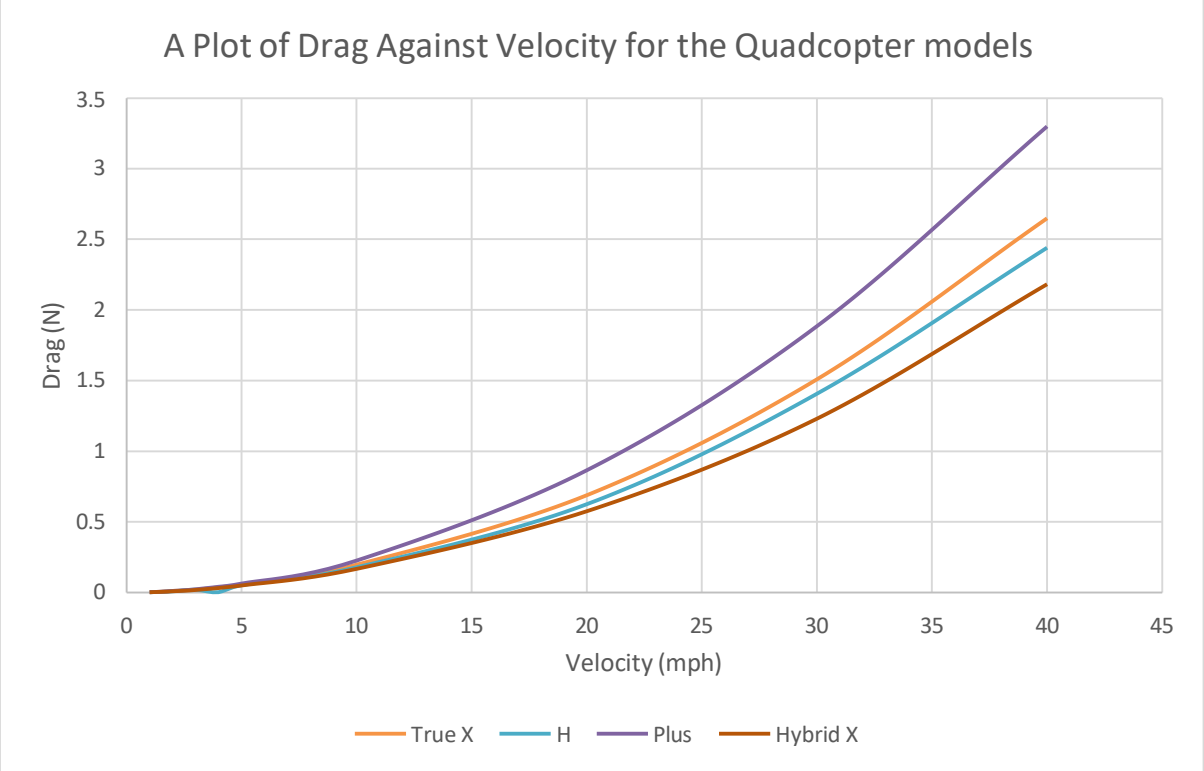

Figure 29 Drag plots for all four quadcopters to compare their drag values.

Based on Figure 29, in spite of the different drag values for each model, there was a general trend: drag increased as velocity increased.

Table 12 shoes the averaged values of drag coefficients of the quadcopter models. The H model had the lowest drag coefficient while the Plus model had the highest.

Model	Cd
True X	0.53165
H	0.40072
Plus	0.54522
Hybrid X	0.41319

Table 12 Drag coefficient values of the quadcopter models.

6.6 Hydrodynamic consideration

In a hydrodynamic study using similar quadcopter models, “Stability and Configuration Study on Amphibious Quadcopter Drones – Water Expert” conducted by Beatriz da Mata Ribeiro, hydrodynamic performance of the quadcopters was simulated. The results obtained are summarized in Figure 30.

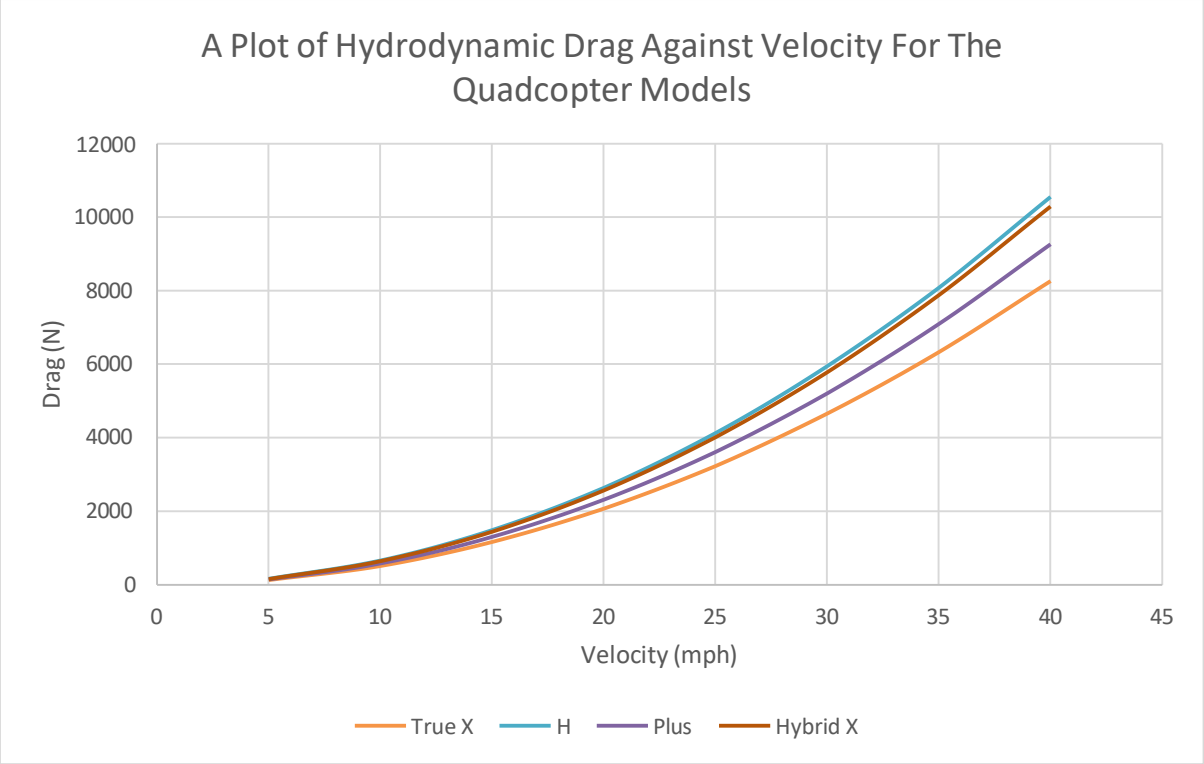

Figure 30 A Plot of hydrodynamic drag for all four models.

7. Conclusion

Even though the H model had the lowest drag coefficient, it did not produce the lowest drag. This is because its shape had a larger effective frontal area which contributes to the drag force acting on it. The hybrid X model had the second lowest drag coefficient but because it had the smallest effective frontal area, it experienced the least drag among the four models. This makes the Hybrid X model the most aerodynamic configuration out of the four models as it moved through air with minimal drag. On the other hand, the True X and Plus models experienced higher values of drag as they had high values of drag coefficients and larger effective frontal area. Despite the two models having drag coefficients that are close in value, the Plus model had a significantly larger effective frontal area resulting in an overall higher drag value than the other configurations.

Therefore, when designing a quadcopter both drag coefficients and effective frontal area need to be considered in optimising the quadcopter design for enhanced aerodynamic efficiency and performance. However, since it is an amphibious quadcopter, the hydrodynamics need to be considered as well. Due to the nature that quadcopters move through water, the effective area and coefficient of drag changes leading to higher drag values. Figure A-23 in Appendix A shows the orientation of a quadcopter moving through water.

A comprehensive study of how quadcopter configuration affects the hydrodynamic performance of the quadcopter is covered in “Stability and Configuration Study on Amphibious Quadcopter Drones – Water Expert" by Beatriz da Mata Ribeiro. From this study, the H model experienced the least amount of hydrodynamic drag compared to the other models while the True X model had the lowest hydrodynamic drag.

In conclusion, the results from the CFD simulations indicate that the shape and configuration of a quadcopter are contributing factors to its aerodynamic performance. Based on both aerodynamic and hydrodynamic performances of the quadcopter, the True X model proves to be an optimal configuration for an amphibious quadcopter. This is because it experiences the lowest hydrodynamic drag which tends to be extremely large compared to aerodynamic drag. Furthermore, the True X does not experience a relatively higher aerodynamic drag compared to the Hybrid X model.

8. Further Development

This project has several potential areas for future work that would help validate it and improve on its accuracy. Such work includes:

1. Experimental work. In addition to the CFD simulations, experimental tests can be conducted to validate the findings. Building physical prototypes of the quadcopters and conducting wind tunnel testing on them can provide empirical data to verify the aerodynamics data from the simulation results. Pressurised water tanks can be used to conduct hydrodynamic experiments to compare with the aerodynamic data.
2. Wake refinement on CFD simulations. Wake refinement is a method used to create a fine mesh behind the model under simulation so that the low velocity wake behind the model is resolved. This would be helpful when simulating at velocities of 5 mph or lower where the wake is not as resolved compared to higher velocity simulations.
3. Structural analysis on quadcopter models using FEA or tensile testing. This would help determine the structural integrity of the quadcopter and its ability to resist stress and strain acting on it in both air and water environments. This would also help in determining the amount of weight that can be carried by the quadcopter frame and the tensile forces on the quadcopter arms and identifying the critical points that experience the most stress. This will aid in designing a structurally robust quadcopter model.
4. Dynamic analysis to assess the quadcopter response to disturbances and manoeuvrability. This would investigate how the different configurations perform under different flight conditions like hovering.

9. Project Management Review

1. *Present the latest version of your Gantt chart and compare it with the initial project plan. What activities demonstrated were critical to the completion of your project? What are the main differences between the two Gantt charts? What adjustments were needed to ensure the successful completion of the project (if any)? Do you think that the estimates made in the initial phase of the project were realistic or optimistic?*

   The most critical parts of the project were CFD simulations on the four quadcopter models and the validation of the CFD methodology. The validation was essential as it established the accuracy of the method used for the CFD simulation. The validated methodology was the one used to conduct all the CFD simulations.

   The major difference between the two Gantt charts is that the initial Gantt chart includes activities and tasks planned for the control of the quadcopter using MATLAB while the final Gantt chart did not include these tasks. Another major difference between the two Gantt charts are the time estimates for the tasks allocated for CFD work. Due to the lengthy CFD work conducted, the timeline for the tasks had to be increased.

   The adjustments needed to ensure the successful completion of the project was the removal of the controls section from the scope of the project.

   Another difference between the two Gantt charts is the additional CAD modelling work that was added to the final Gantt chart. Due to errors brought by the initial CAD model used in the project, new CAD models had to be designed from scratch using CATIA.

   The estimates made in the initial phase of the project were optimistic. The lengthy CFD work took more time than was expected and more errors were encountered than what was expected. Even though the initial estimates included buffer weeks to accommodate any unexpected delays, these were insufficient, and more time had to be spent on the CFD work.

2. *Explain and justify the key changes (if any) that affected the project plan. What key changes did you make to your project time plan to ensure the timely and successful completion of your project? What was/were the reason(s) behind each change? What was the impact of such changes on the entire project plan?*

   There were two key changes that affected the project plan: designing and creating quadcopter models and the removal of control systems part of the project.

   At first, a ready-made quadcopter model from the internet was used. The design had a True X configuration, and a few changes were to be made to the design of the arms to create the remaining three configurations. However, this was unsuccessful due to the complicated and poorly designed model. Instead, new models were made from scratch on CATIA as explained in Section 3. Due to these problems and changes, the CFD work had to be delayed since CFD simulations could not take place without the models.

   Changes to CFD setup: At first, the CFD work had to be delayed due to errors and problems in CAD modelling, but the CFD simulations took a longer time to set-up and run than the anticipated time. Initially, during the CFD setup, a freestream sphere was to be used as the boundary layer as

this would have allowed an easier change in the angle of attack for the quadcopter. However the use of freestream brought up several errors and problems, some of which could not be solved in time to complete the project. Therefore, a boundary block was used instead of the freestream sphere. Additionally, there were several problems with the software itself as it was unable to recognise the quadcopter assembly as a single body part rather it identified it as seven separate parts making the Boolean operation unsuccessful. This was resolved by making CAD repairs on Star CCM+ to unite the body parts into one. This process further delayed the CFD work.

Due to the significant CFD delays, the scope of the project had to be redefined and the control systems part was removed completely.

3. *Reflect on the strengths and weaknesses of the management of the process. What are your strengths and weaknesses as a project manager? What aspects of the management of your project are you particularly satisfied with? What could have been improved? If you were to start the project again, what would you be doing differently?*

   One of the project manager's strengths was problem solving and resourcefulness. Throughout the project, a lot of problems and errors were encountered especially during CFD simulations. Most of these problems were solved by with the help of online articles, project reports, help from the supervisor and trial and error method. For instance, when importing the quadcopter model, Star CCM+ identified the model as an assembly with seven separate body parts instead of one body part. This in turn made it difficult to perform the Boolean subtract operation on the model. To solve this, the quadcopter model had to be imported to the CAD modelling section packaged within Star CCM+, where the body parts were united into one. The body part generated from this was successful in performing the Boolean subtract operation.

   One of the weaknesses of the project manager was time management. The initial estimates and allocated times for most of the tasks were too optimistic. A lot of time was spent learning the Star CCM+ software and trying to solve the errors encountered in the project. For example, a significant amount of time was used in trying to solve the problems faced during CAD modelling of the ready-made quadcopter model before it was decided, as an alternative, to design the models from scratch which took less time than expected.

   A satisfying aspect of the project management was the ability to make necessary adjustments to the project so that it could be delivered properly and on time. For instance, adjusting the scope of the project allowed the timely completion and delivery of the project.

   An improvement for the project management is to set deadlines for problem solving and identifying deadlock errors. Instead of spending weeks trying to solve the problems that were deadlocked and unsolvable, alternative options should have been used earlier in order to stay on track with time.

   If the project were to be restarted, time management would be done differently. More realistic timelines would have been allocated to the project tasks and more time would be allocated to learning and understanding Star CCM+ in depth.

4. *Improvements to be considered in terms of time management. If you were to start this project again, how would you improve the time management of the project? What changes would you consider in your project planning and/or time management?*

   If the project were to be restarted, more realistic timelines would be used for the project tasks and less time would be used in solving problematic errors that could be solved by changing the methodology. More time would be allocated to the CFD tasks like set-up and post processing and the simulations of the quadcopter models would be run parallel since none of the simulations depended on each other to solve.

.

10. Quality management

1. *Identify and critically discuss the role of relevant standards in relation to your project. What is the role played by standards in relation to you project? What is the difference between standards and regulations? How does this affect the engineering practice? Could you provide examples of relevant standards and/or regulations that need to be considered and/or inform your work?*

   The major role played by standards in relation to this project is ensuring the accuracy of the simulation results by conducting a mesh sensitivity study that analyses how the generated mesh affects the results produced.

   Standards are rules or guidelines that offer suggestions for best practice, these are not enforceable by law [16], [14]. Regulations on the other hand, are rules that must be followed for legal or safety purposes, these are legally binding and must be adhered to [16],[14].

   Standards and regulations help in ensuring that engineering products and services are of acceptable quality, consistency, safety and compatibility.

   Standards like the ISO/TS 10303-1375:2014-02 give rules and guidelines on CFD simulations. These guidelines include geometric sensitivity, mesh sensitivity [17], boundary conditions [18], physics model and convergence [15].

2. *Critically discuss the advantages and disadvantages that arise from the adoption of quality standards in relation to your project in business environment. What are the main advantages of adopting specific quality standards? What are the disadvantages? In your opinion, do the advantages outweigh the disadvantages? Justify your answer, considering the results of your discussion.*

   Adopting quality standards in the CFD simulation of quadcopters ensures a high level of accuracy that strengthens the integrity of the results. They also provide guidelines on how to conduct a proper and accurate CFD simulation. Conversely, some quality standards may be unsuitable for quadcopter CFD work, leading to time-consuming errors.

   The advantages of quality standards outweigh the disadvantages. Quality standards provide assurance on the quality of the CFD work undertaken and can have long-term advantages for the business. The disadvantages can be solved by having a thorough selection process while selecting the standards to apply to the CFD simulation.

3. *Using your logbook as a reference, identify within your project, areas for improvement, areas that might be subjected to standards and regulations (including safety and ethical concerns) and purpose appropriate ideas and solutions to improve or mitigate against in the outcome. What aspects of your project could be further improved? What solutions could be considered?*

   An area for improvement based on the logbook entries is planning and preparing for CFD simulations. Even though the CFD simulations were lengthy, most f them can be run parallel in order to save time.

The areas that might be subjected to standards and regulations are mesh analysis and boundary layer and conditions setup.

One of the project aspects to improve further is wake refinement, especially for the simulation performed at low velocities. Wake refinement will enable the low velocity wake behind the quadcopter models to resolve properly.

REFERENCES

[1] Aviastar, “Breguet-Richet Gyroplane No.1,” [Online]. Available: https://www.aviastar.org/helicopters_eng/breguet_gyro.php.

[2] Drone AG, “DJI Agras: Automated Crop Spaying Drone,” 2024. [Online]. Available: https://droneag.farm/solutions/dji-agras-spraying-drone/.

[3] Krossblade Aerospace, “History of Quadcopters and Other Multirotors,” [Online]. Available: https://www.krossblade.com/history-of-quadcopters-and-multirotors. [Accessed March 2024].

[4] B. S. C. K. F. K. V. O. M. R. C. T. Komal SA Khuwaja, “Vrtual Reality Based Visualization and Training of a Quadcopter by Using RC Remote Control Transmitter,” 2018. [Online]. Available: https://iopscience.iop.org/article/10.1088/1757-899X/444/5/052008. [Accessed March 2024].

[5] Siemens, “What is CFD Simulation,” [Online]. Available: https://www.plm.automation.siemens.com/global/en/our-story/glossary/cfd-simulation/67873. [Accessed 10th October 2023].

[6] Simscale, “What is CFD | Computational Fluid Dynamics,” 7th December 2023. [Online]. Available: https://www.simscale.com/docs/simwiki/cfd-computational-fluid-dynamics/what-is-cfd-computational-fluid-dynamics/. [Accessed March 2024].

[7] theansweris27.com, “Physics models in STAR-CCM+ (Part IV: turbulence models),” [Online]. Available: https://theansweris27.com/physic-models-in-star-ccm-part-iv/.

[8] S. Solmaz, “Turbulence: Which Model Should I Select For My CFD Analysis,” 13th March 2024. [Online]. Available: https://www.simscale.com/blog/turbulence-cfd-analysis/.

[9] Siemens, “A new user's guide to Simcecter STAR-CCM+ simualtion(Part 4/5): Physics setup and Solvers,” 25 March 2021. [Online]. Available: https://community.sw.siemens.com/s/article/A-new-user-s-guide-to-STAR-CCM-simulation-Part-4-5-Physics-setup-and-Solvers. [Accessed November 2023].

[10] Siemens, “A new user's guide to Simcenter STAR-CCM+ simulation (Part 3/5): Meshing,” 25 March 2021. [Online]. Available: https://community.sw.siemens.com/s/article/A-new-user-s-guide-to-STAR-CCM-simulation-Part-3-5-Meshing. [Accessed November 2023].

[11] CENTAUR Software, “Prismatic Elements in the Boundary Layer,” [Online]. Available: https://www.centaursoft.com/prism-layers. [Accessed November 2023].

[12] Ideal Simulations, “CFD Mesh guide,” [Online]. Available: https://www.idealsimulations.com/guides/cfd-mesh-guide/#:~:text=1)%20Base%20cell%20size%3A%20this,the%20cell%20size%20is%20halved. [Accessed November 2023].

[13] NASA - Glenn Research Center, “Shape Effects on Drag,” [Online]. Available: https://www.grc.nasa.gov/www/k-12/VirtualAero/BottleRocket/airplane/shaped.html. [Accessed February 2024].

[1 RISK AND RESILIENCE Hub, “Do you know the difference between standards and regulations?,”
4] 20th January 2019. [Online]. Available: https://www.riskandresiliencehub.com/do-you-know-the-difference-between-standards-and-regulations/. [Accessed March 2024].

[1 Altair AcuSolve, “Guidelines for Quality CFD Modeling,” 2023. [Online]. Available:
5] https://help.altair.com/hwcfdsolvers/acusolve/topics/acusolve/training_manual/guidelines_for_cfd_modeling_r.htm. [Accessed December 2023].

[1 ASQ, “What Are Quality Standards?,” [Online]. Available: https://asq.org/quality-resources/learn-
6] about-standards. [Accessed March 2024].

[1 Altair AcuSolve, “Mesh Sensitivity,” [Online]. Available:
7] https://help.altair.com/hwcfdsolvers/acusolve/topics/acusolve/training_manual/mesh_sensitivity_r.htm#reference_olf_1x3_pw. [Accessed November 2023].

[1 Altair AcuSolve, “Boundary Condition Sensitivity,” [Online]. Available:
8] https://help.altair.com/hwcfdsolvers/acusolve/topics/acusolve/training_manual/bc_sensitivity_r.htm. [Accessed November 2023].

[1 C. Allison, “Meshing in FEA: Mesh convergence,” Onscale, 12th June 2020. [Online]. Available:
9] https://onscale.com/meshing-in-fea-mesh-convergence/#:~:text=The%20process%20of%20mesh%20convergence,sampled%20across%20its%20physical%20domain.. [Accessed November 2023].

[2 NASA - Glenn Research Center, “The Drag Equation,” [Online]. Available:
0] https://www.grc.nasa.gov/www/k-12/VirtualAero/BottleRocket/airplane/drageq.html. [Accessed January 2024].

BIBLIOGRAPHY

1. Anderson JD. Fundamentals of Aerodynamics. 2001.
2. Bertin JJ, Smith ML. Aerodynamics for Engineers. 1988.

APPENDIX A

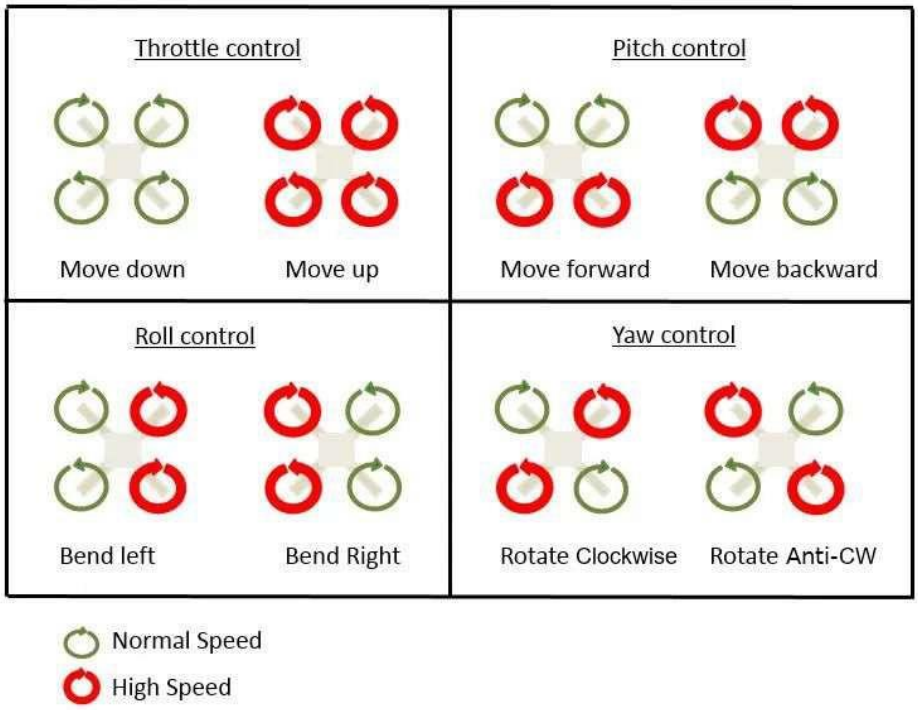

Figure A - 1 Thrust variation on motors used to achieve quadcopter motion.

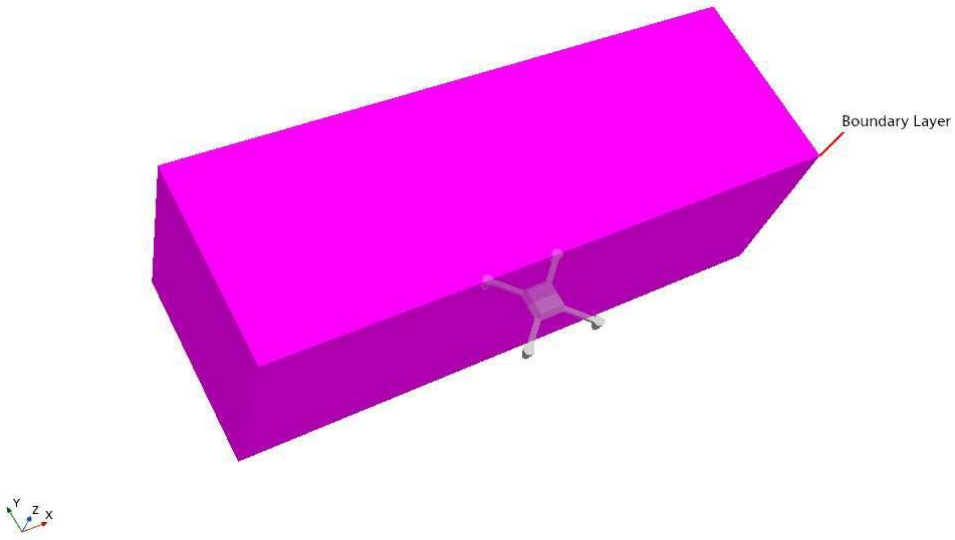

Figure A - 2 Boundary block surrounding half of the quadcopter model.

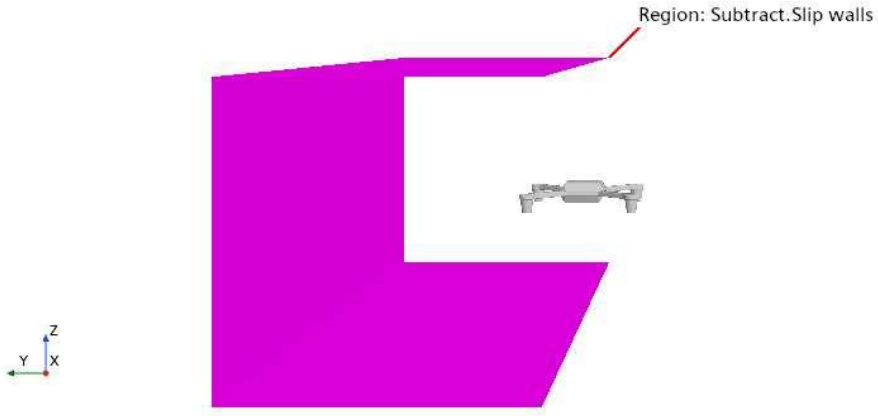

Figure A - 3 Slip walls for the boundary layer.

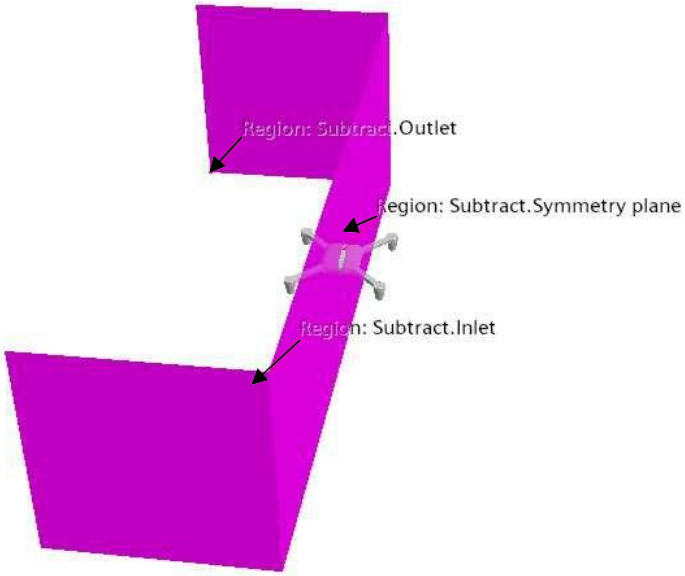

Figure A - 4 Outlet, inlet and symmetry plane surfaces of the boundary block.

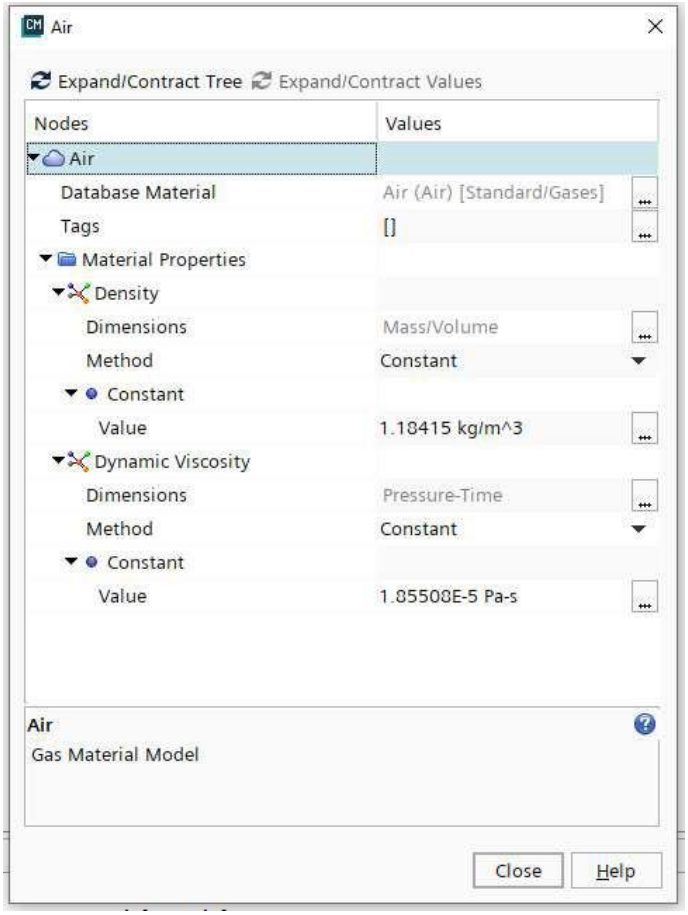

Figure A - 5 Fluid properties used in the CFD simulations.

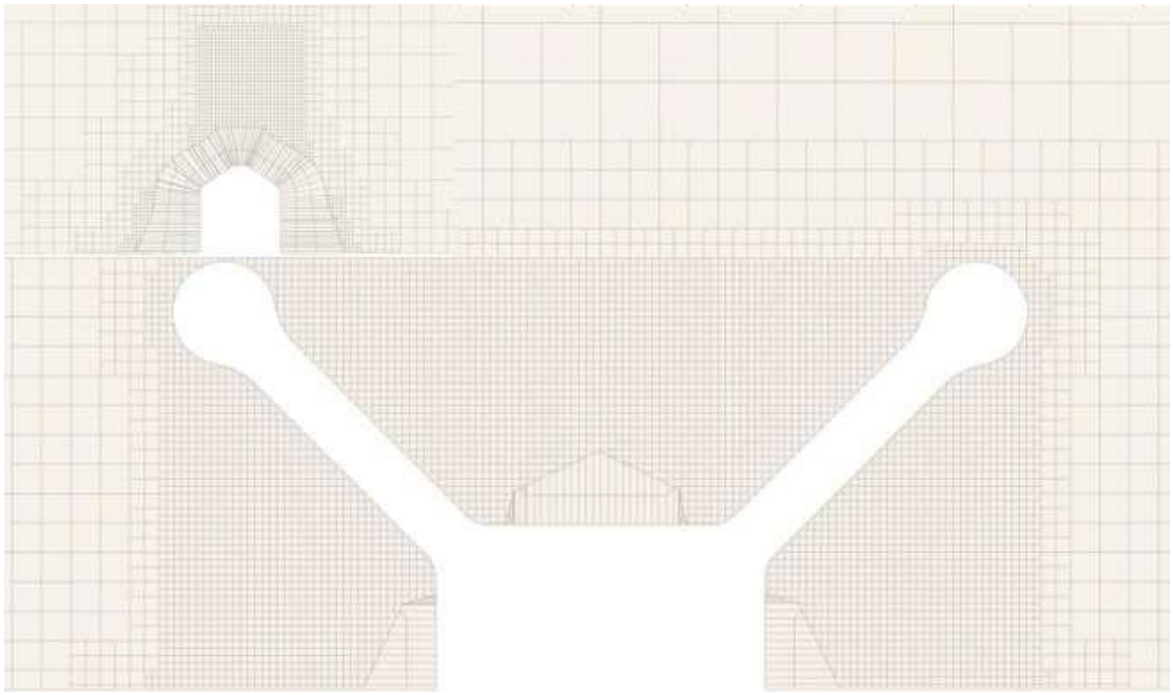

Figure A - 6 Mesh visualisation at 0.5m base size and 3 prism layer with 33.33% thickness.

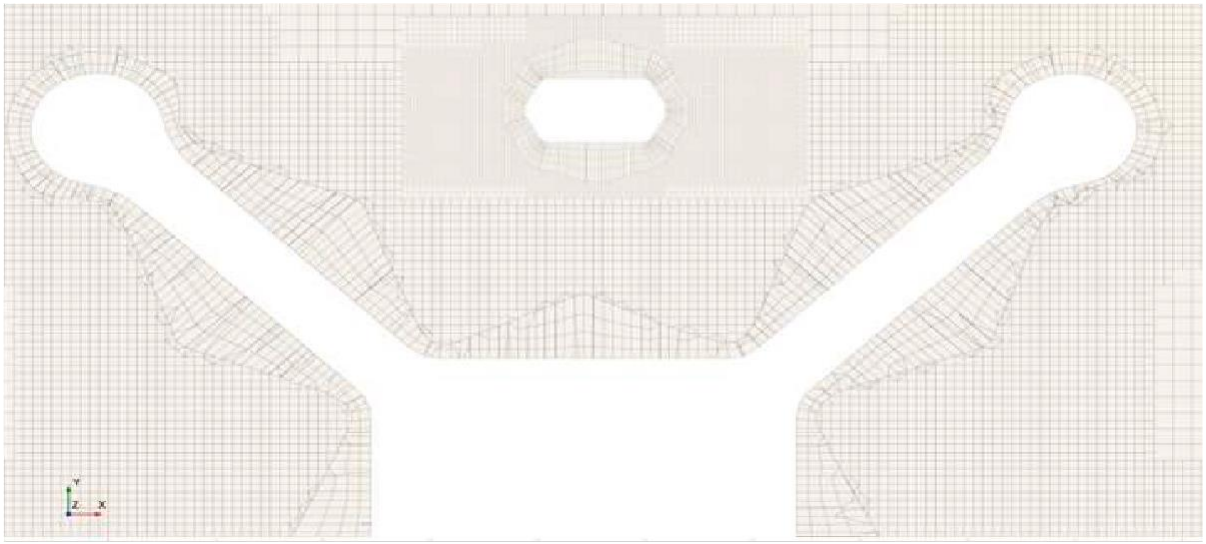

Figure A - 7 Mesh visualisation at 0.5m base size and 4 prism layers with 5% thickness.

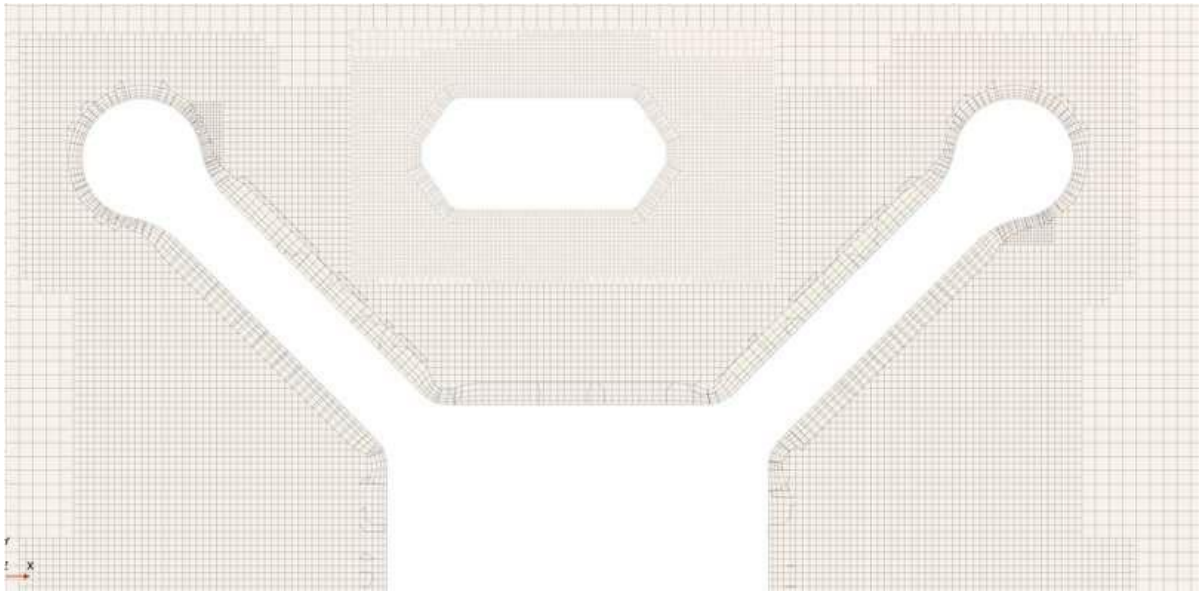

Figure A - 8 Mesh visualisation at 0.4m base size and 4 prism layers with 2.5% thickness.

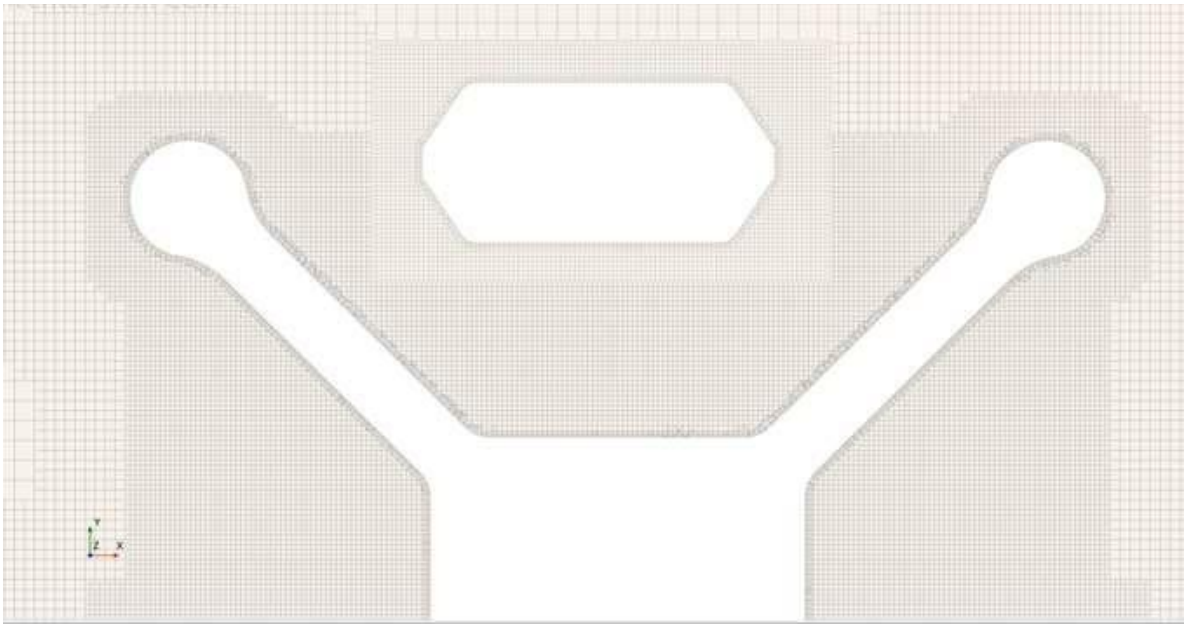

Figure A - 9 Mesh visualisation at 0.3m base size and 4 prism layers with 1% thickness.

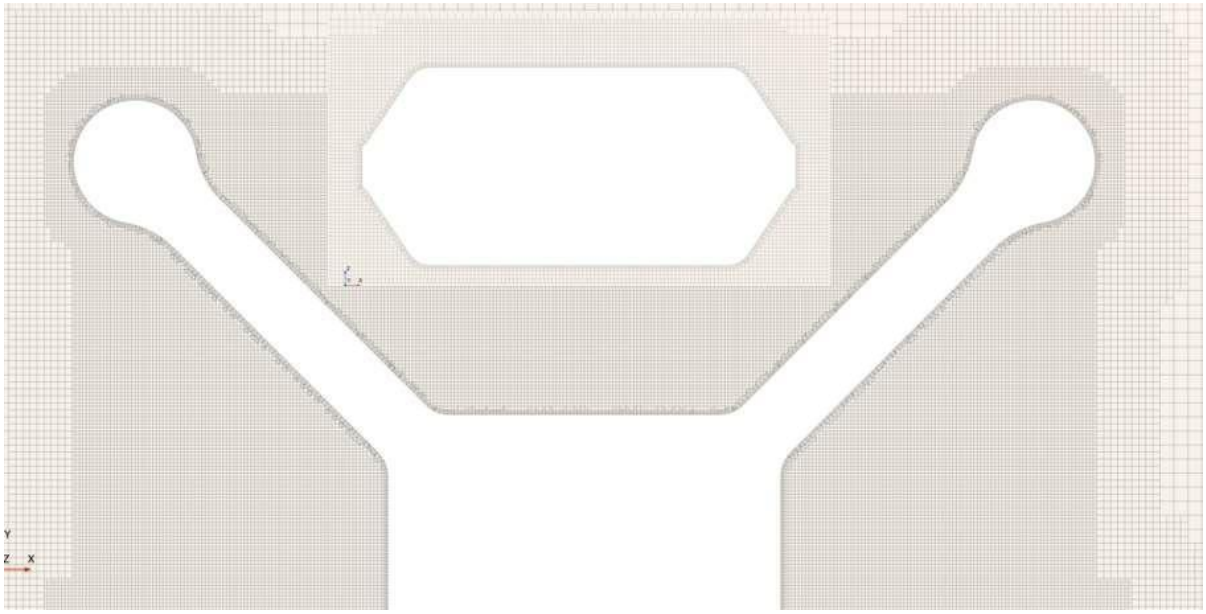

Figure A - 10 Mesh visualisation at 0.2m base size and 4 prism layers with 1% thickness.

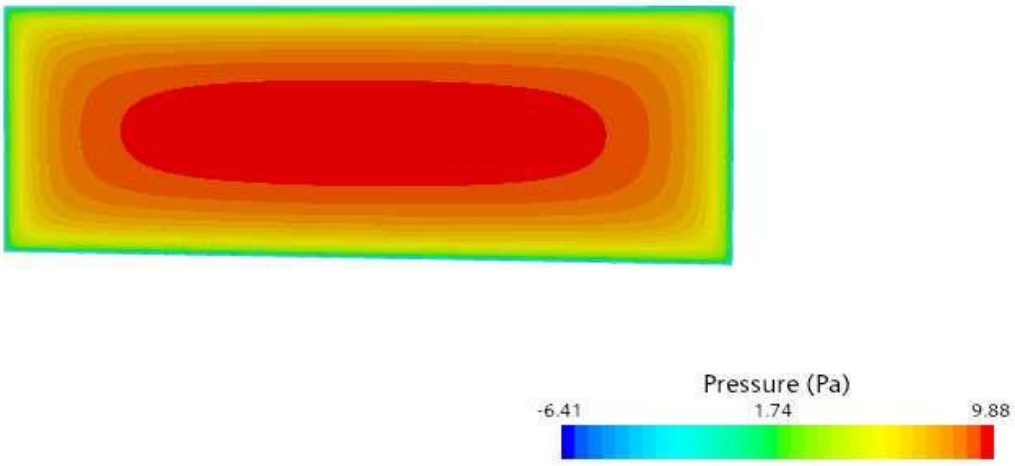

Figure A - 11 Pressure distribution on the front face of the flat plate.

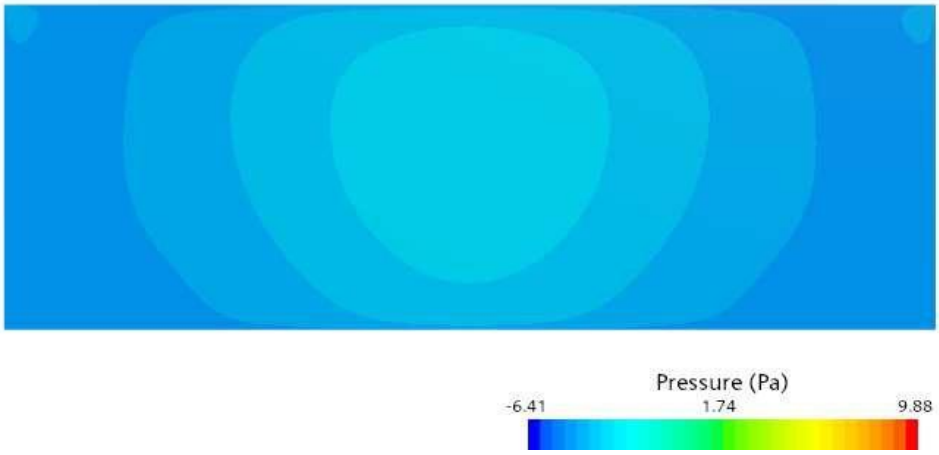

Figure A - 12 Pressure distribution on the back face of the flat plate.

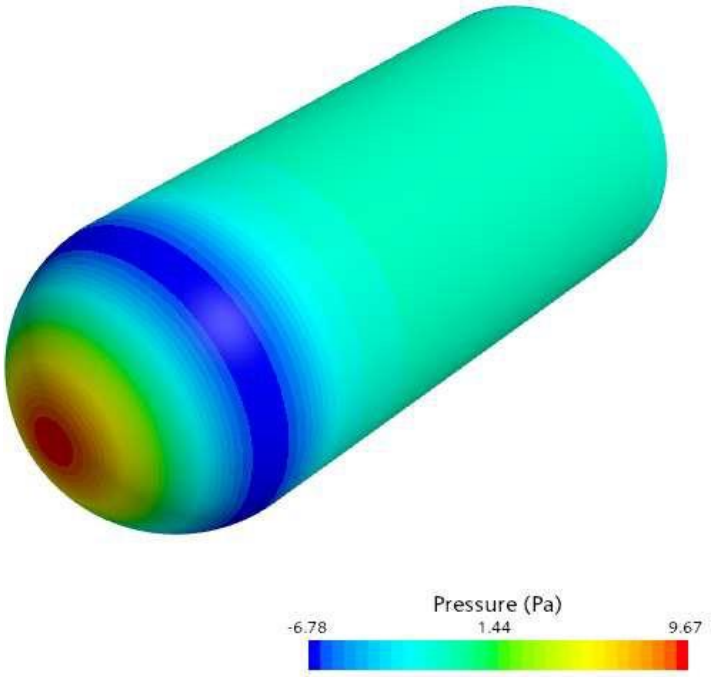

Figure A - 13 Pressure distribution on the bullet validation model.

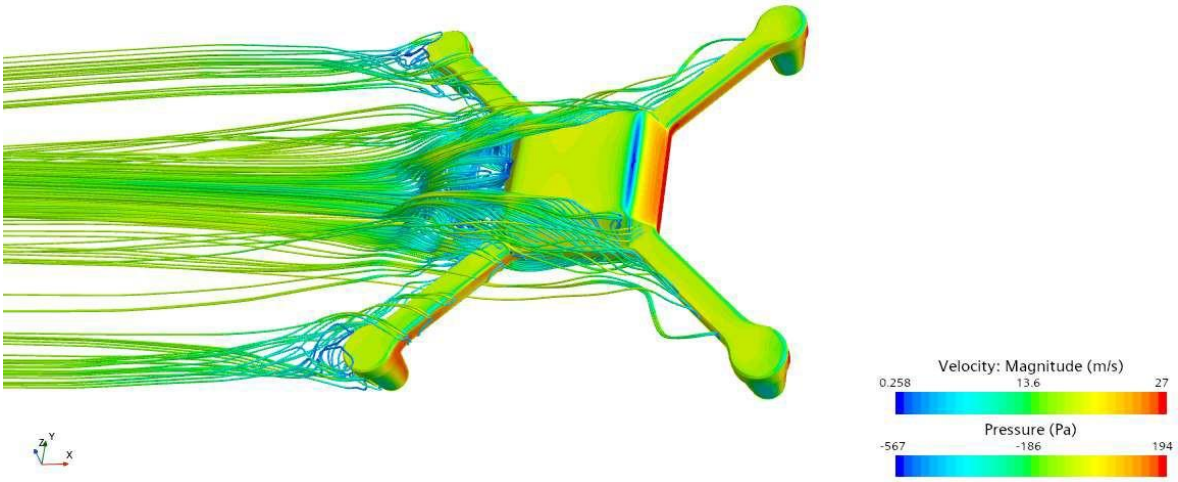

Figure A - 14 Pressure distribution and velocity streamlines for the True X model at 40mph.

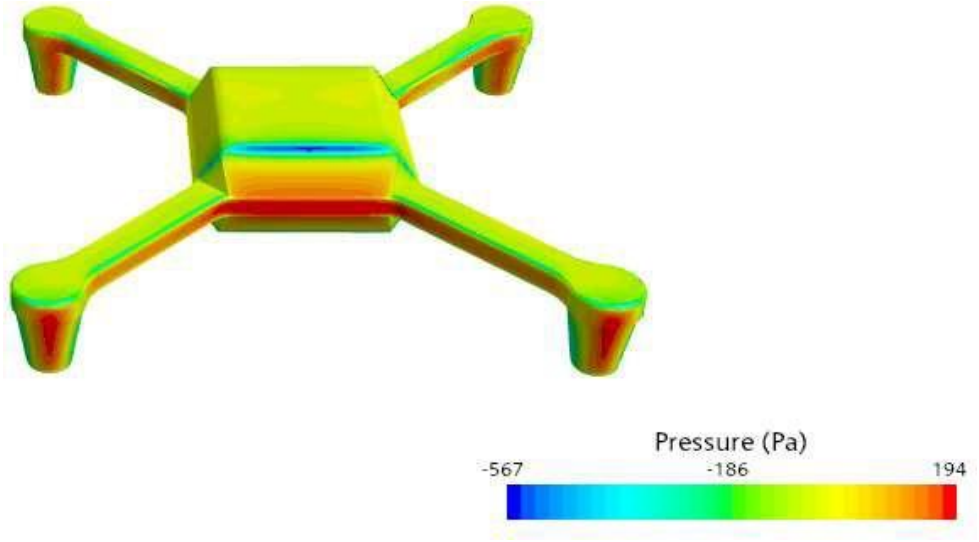

Figure A - 15 Pressure Distribution on the True X model at 40mph.

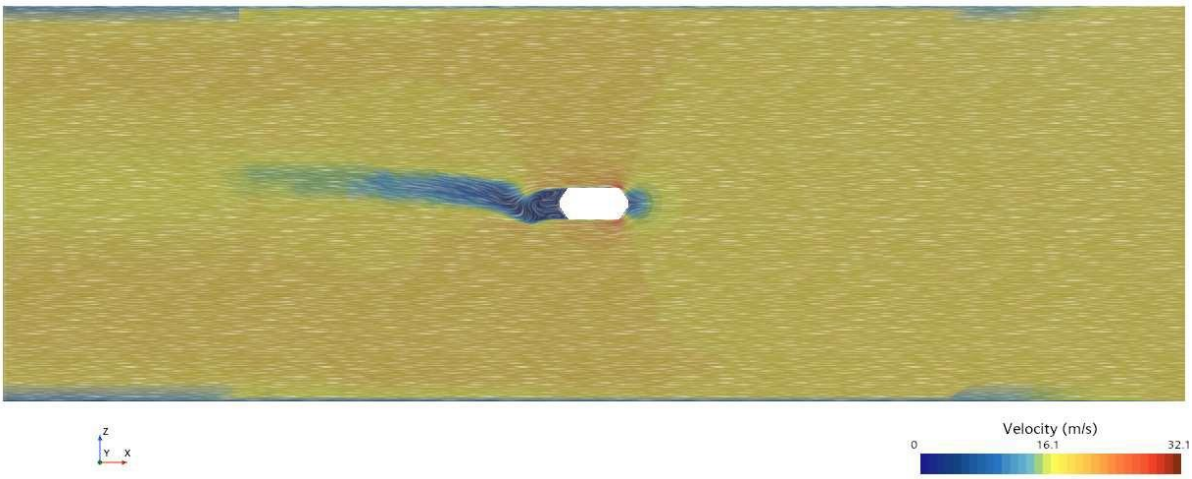

Figure A - 16 Airflow field surrounding the True X model at 40mph.

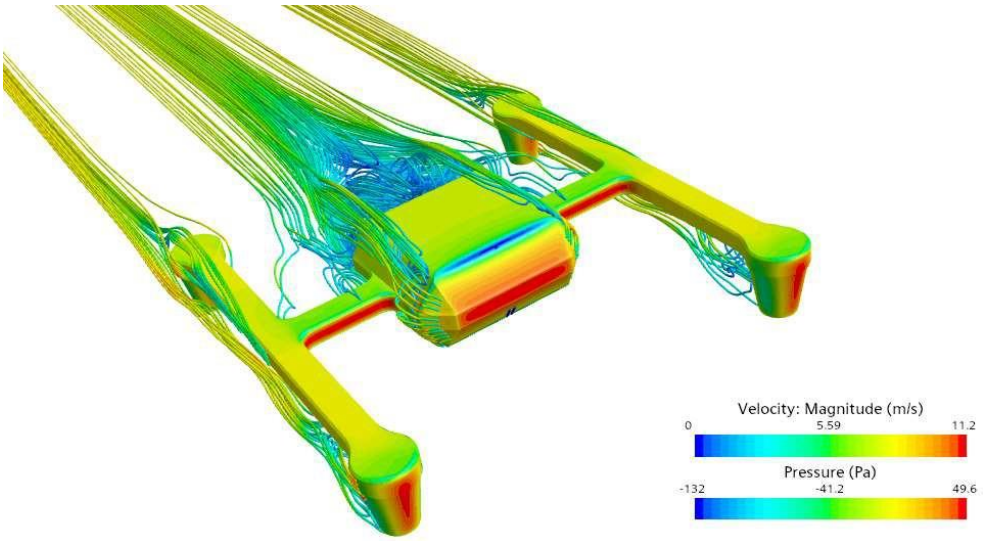

Figure A - 17 Pressure distribution and velocity streamlines for the H model at 20mph.

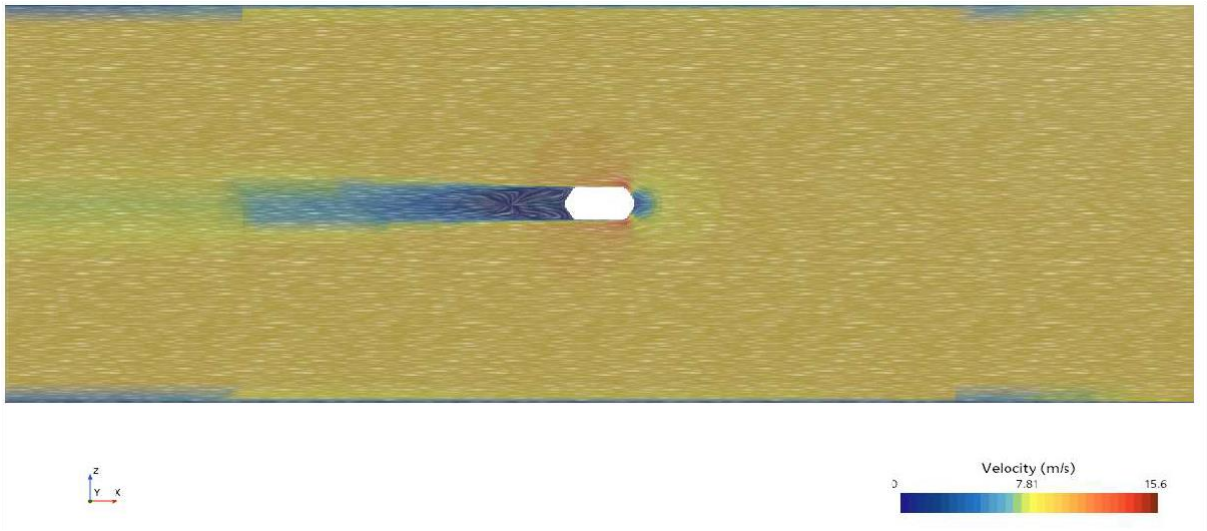

Figure A - 18 Airflow field surrounding the H model at 20mph.

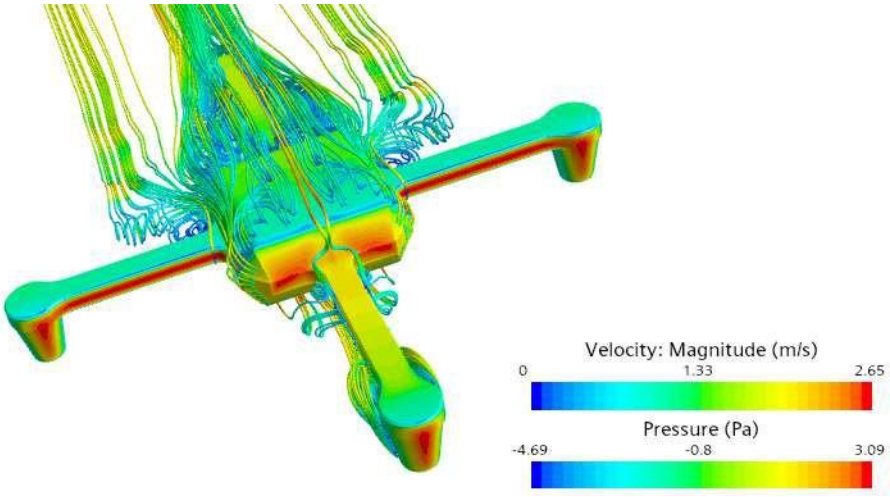

Figure A - 19 Pressure distribution and velocity streamlines for the Plus model at 5mph.

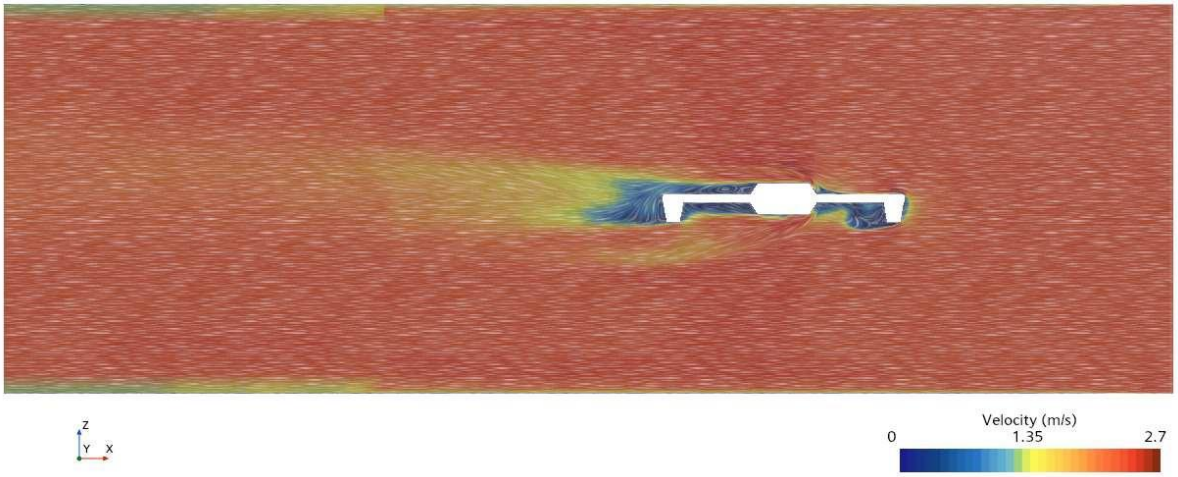

Figure A - 20 Airflow field surrounding the Plus model at 5mph.

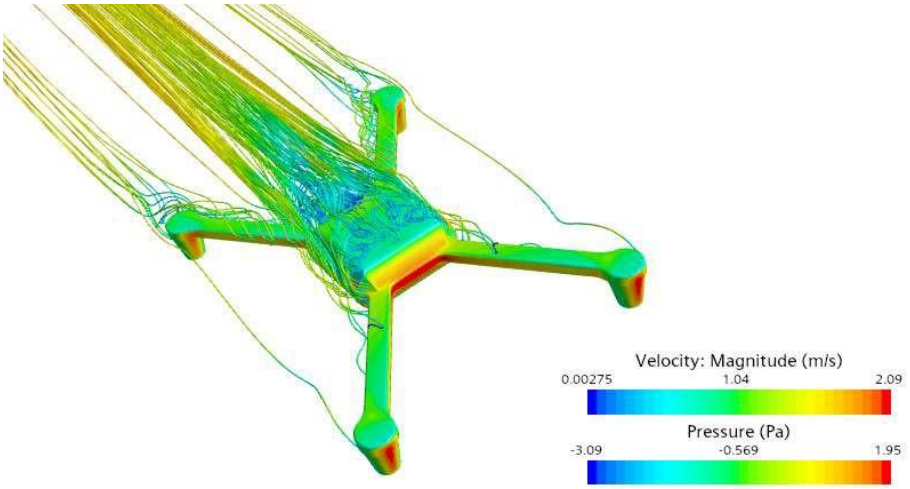

Figure A - 21 Pressure distribution and velocity streamlines for the Hybrid X model at 4mph.

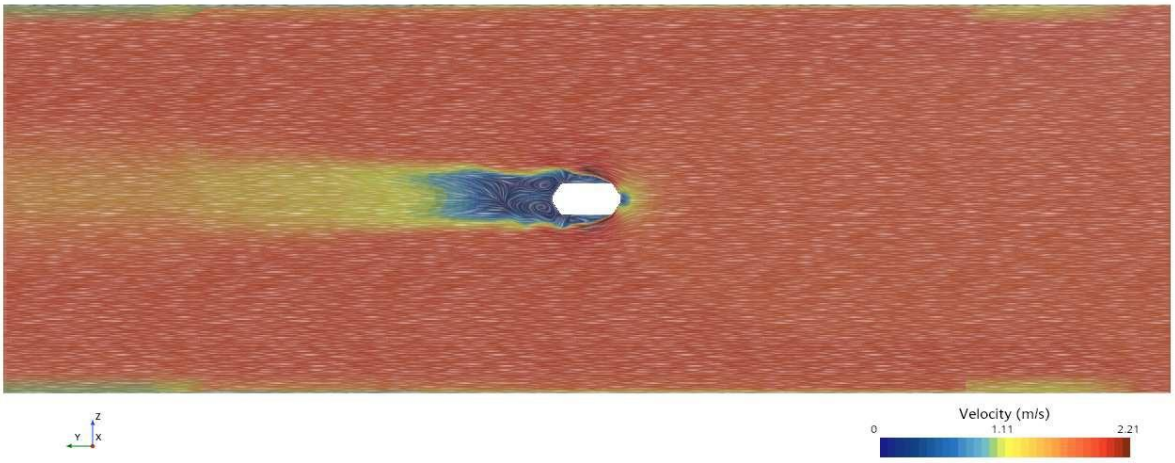

Figure A - 22 Airflow field surrounding the Hybrid X model at 4mph.

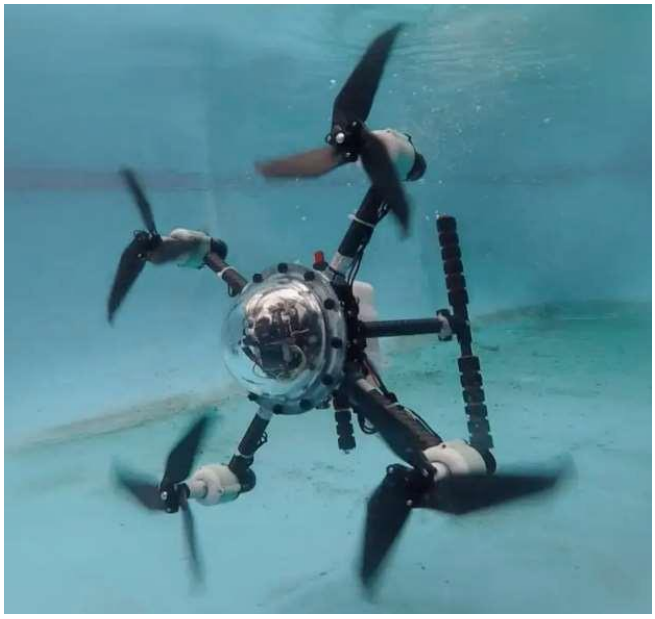

Figure A - 23 Quadcopter orientation as it moves through water.

APPENDIX B

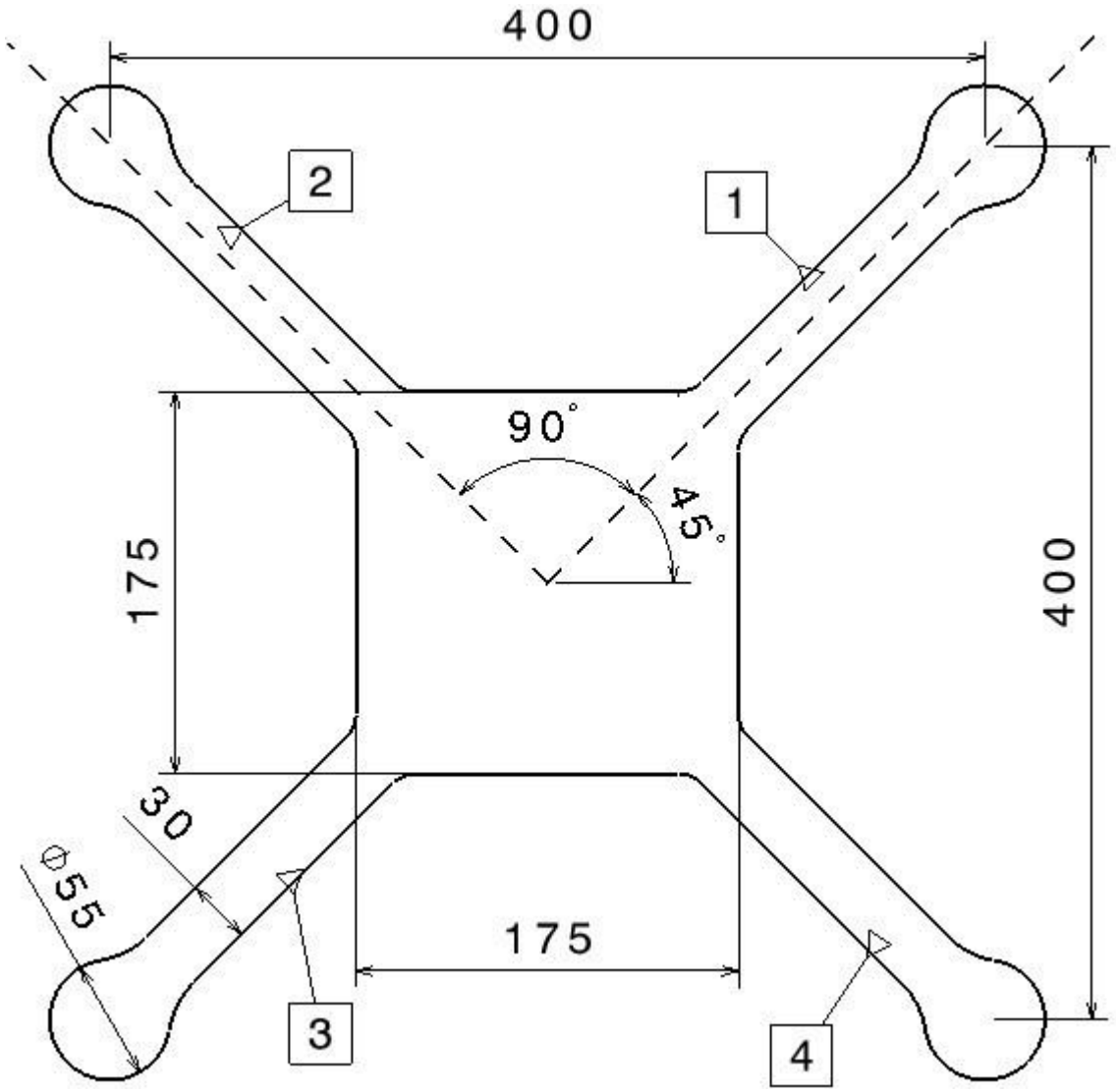

Figure B - 1 True X sketch showing dimensions used to create the arms.

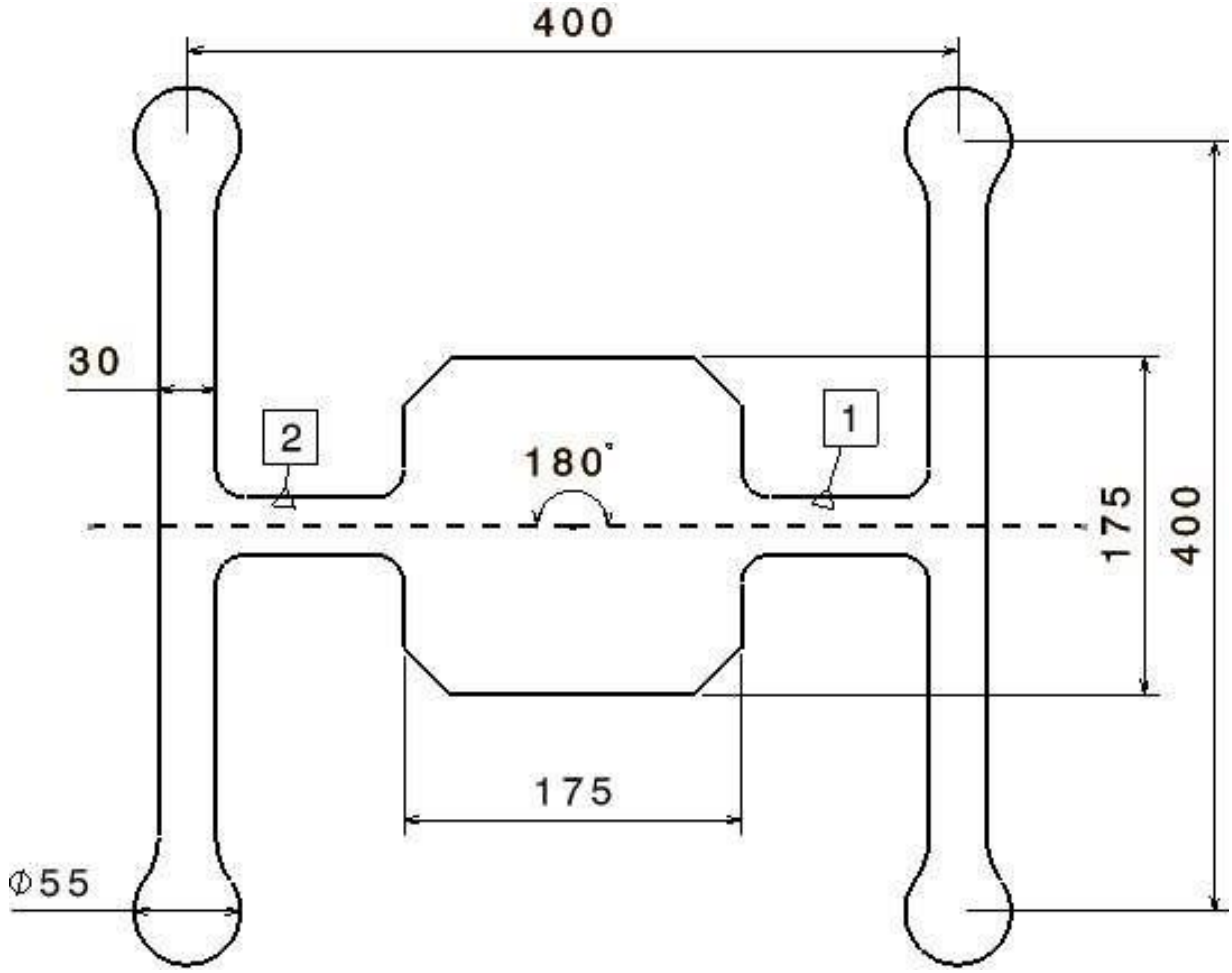

Figure B - 2 H model sketch showing dimensions used to create the arms.

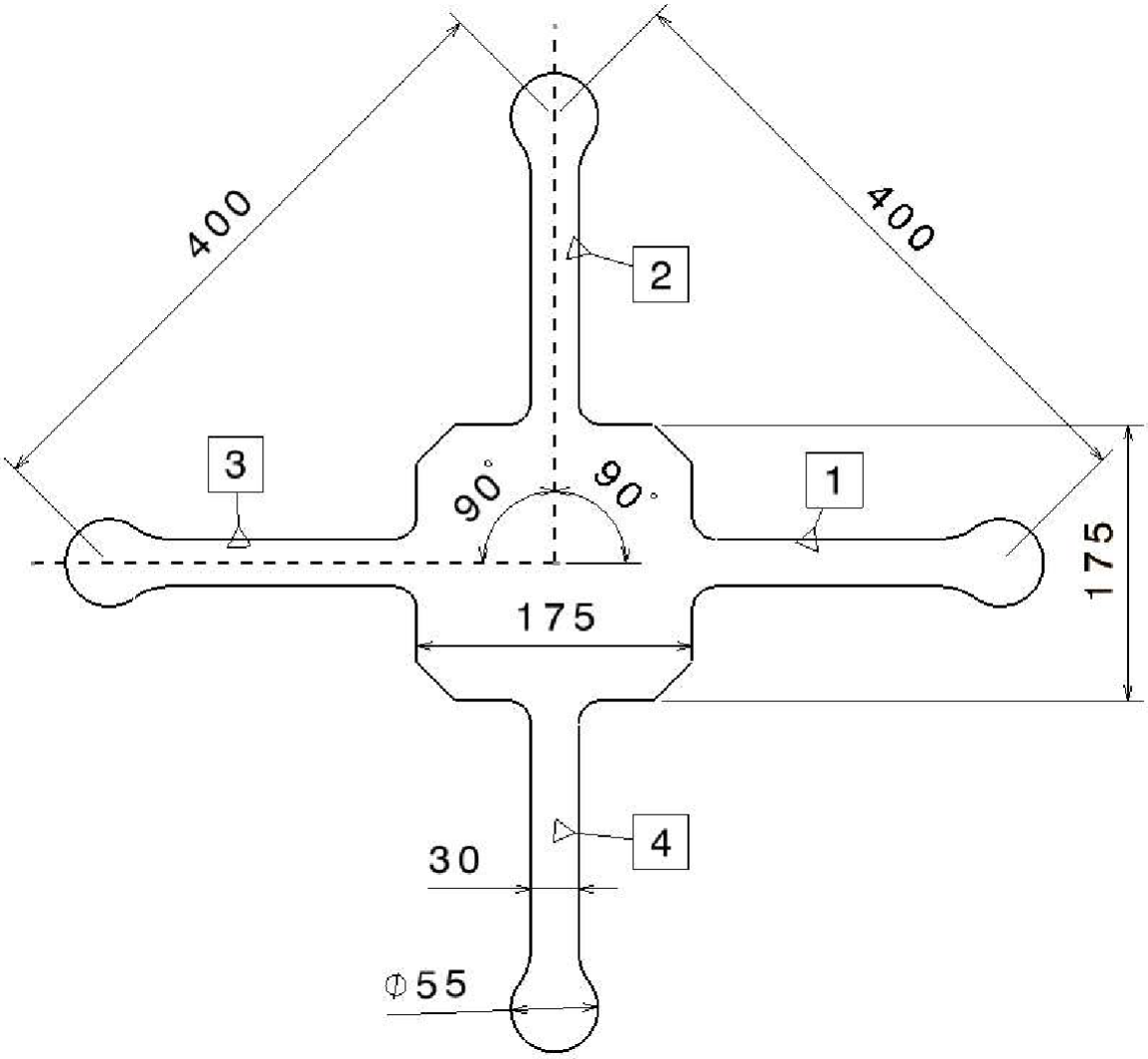

Figure B - 3 Plus model sketch showing dimensions used to create the arms.

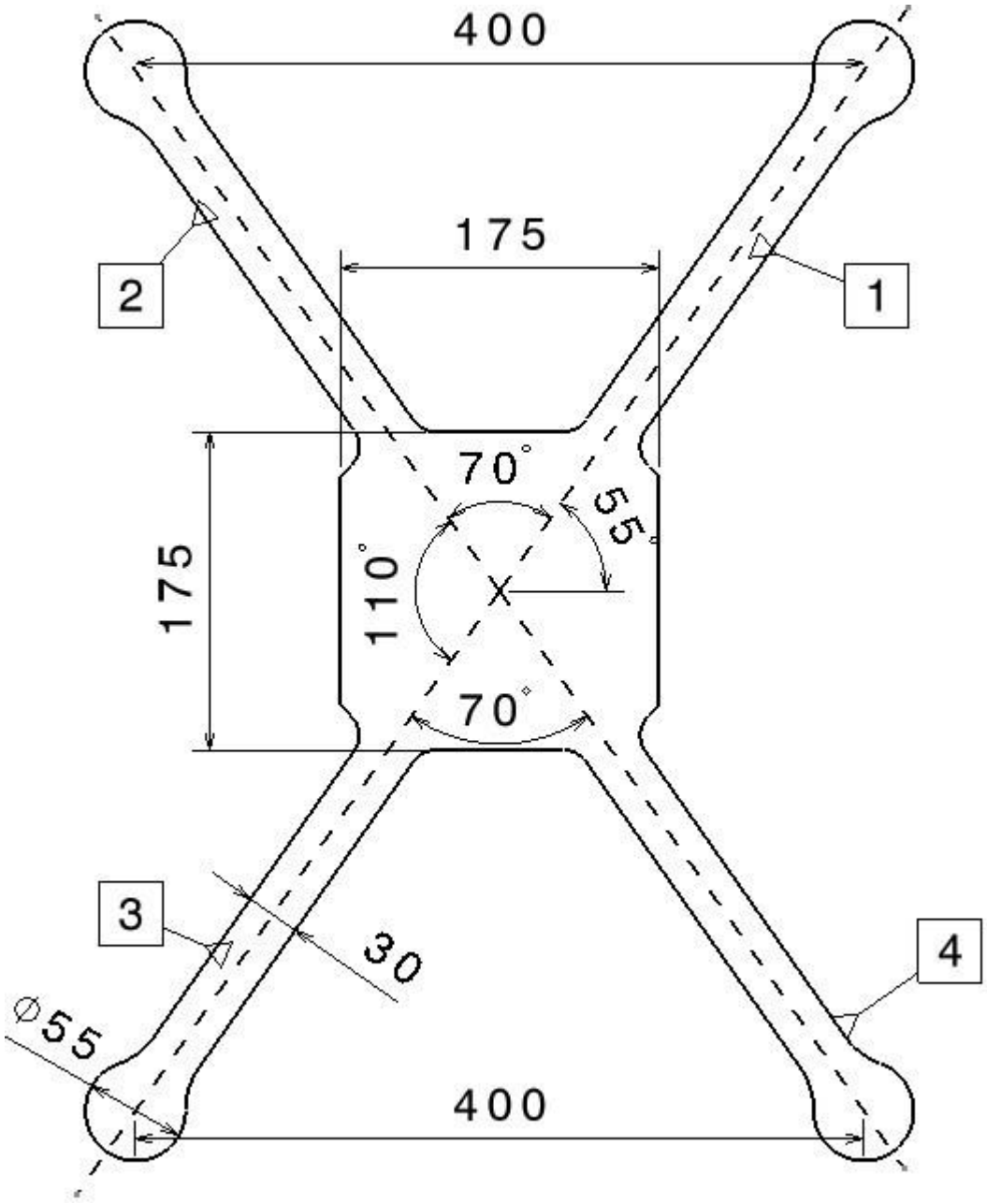

Figure B - 4 Hybrid X sketch showing dimensions used to create the arms.

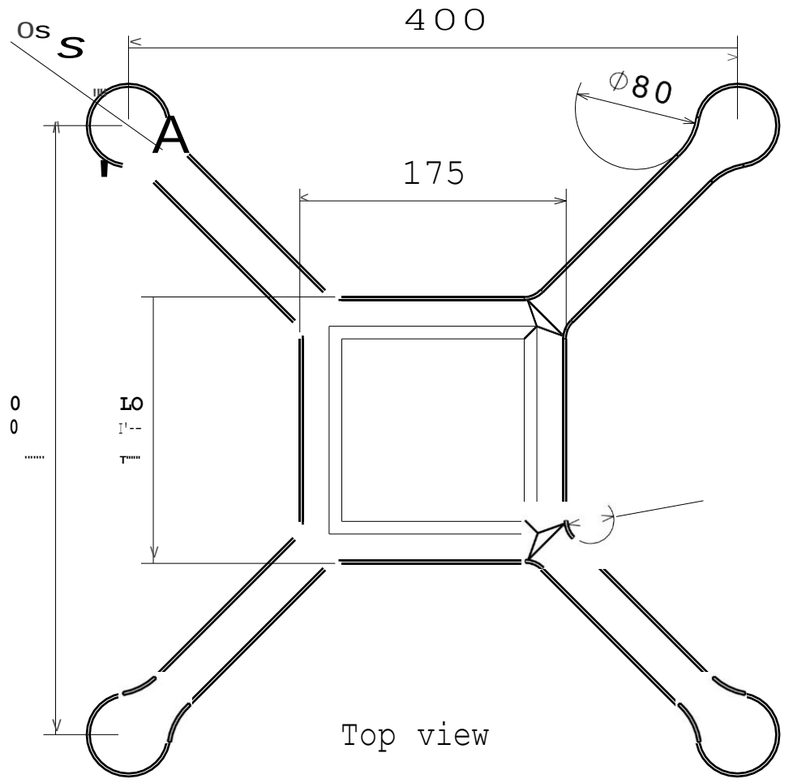

Top view

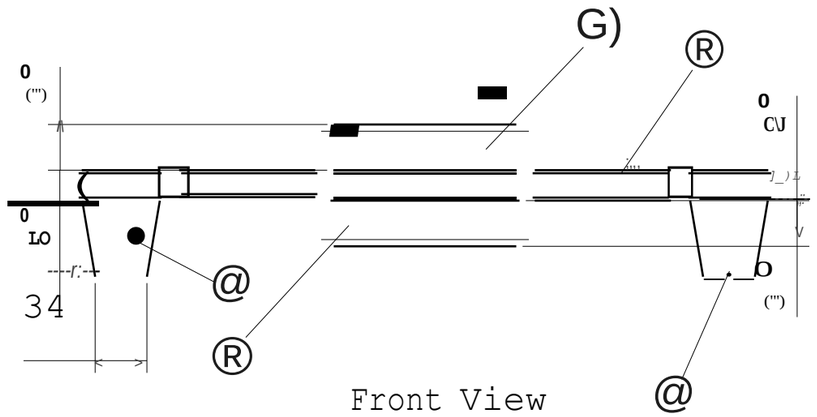

Front View

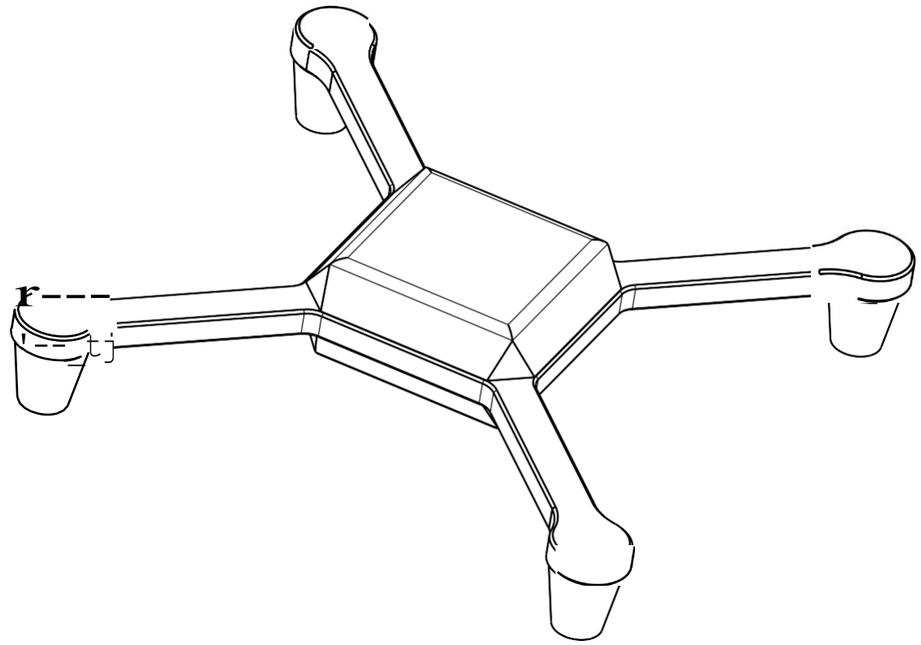

Isometric view

Part Number	Part Name
1	Top body part
2	Bottom body part
3	True X middle layer
4	Quadcopter feet

NOTE:
1. The four faces on the top and bottom body parts have a face draft of 34 degrees.
2. The four corners on the top and bottom body parts, each have a draft of -17 degrees.
3. The middle layer with the arms has an edge fillet of 15 mm.

DRAWN BY: Roselyn Kissaka DATE: NOVEMBER 2023	TRUEX ASSEMBLY		
CHECKED BY: Roselyn Kissaka DATE: NOVEMBER 2023			
smA3	CJ©	UNIVERSITY OF HERTFORDSHIRE	
SCALE: 1:4	WEIGHT (kg): 2.77	LOCATION: APPENDIX B	SHEET: 1/4

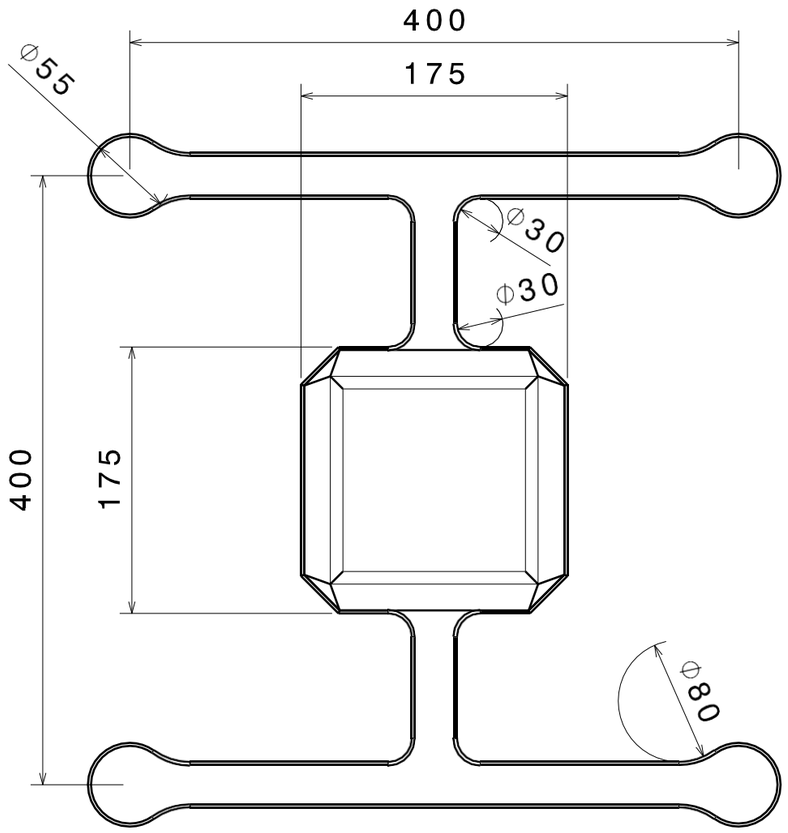

Top View

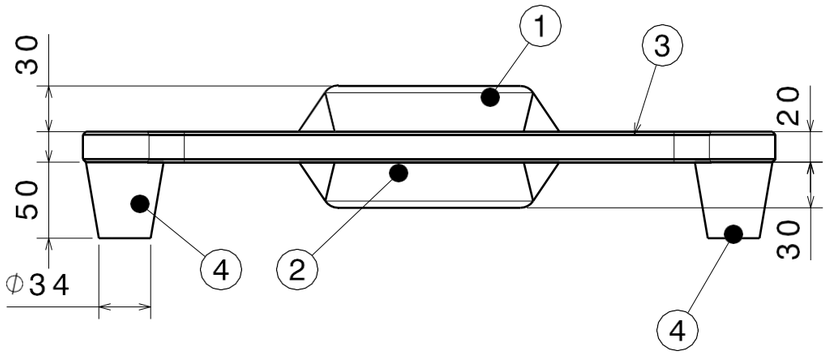

Front View

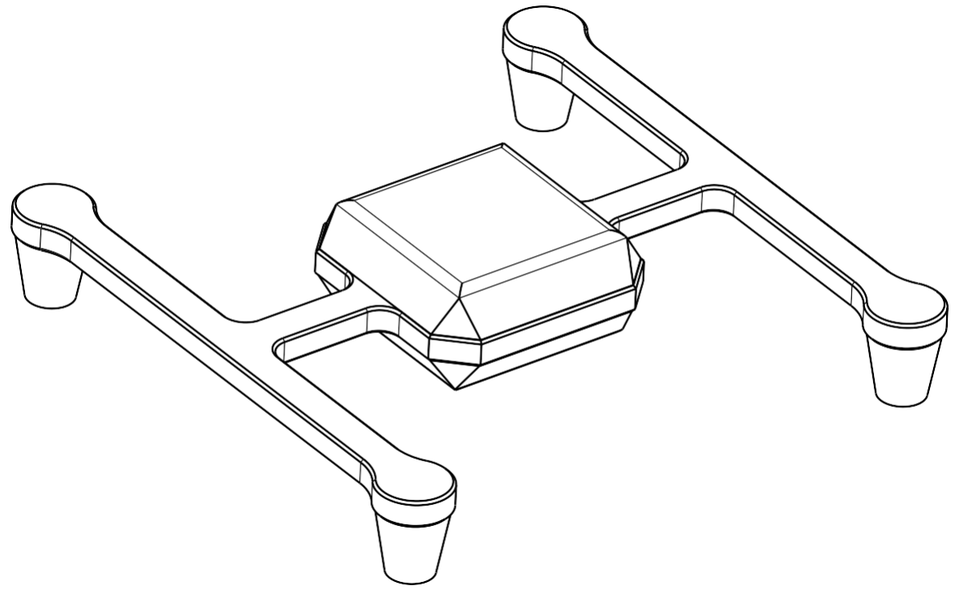

Isometric view

Part Number	Part Name
1	Top body part
2	Bottom body part
3	H middle layer
4	Quadcopter feet

NOTE:
1. The four faces on the top and bottom body parts have a face draft of 34 degrees.
2. The four corners on the top and bottom body parts, each have a draft of -17 degrees.
3. The middle layer with the arms has an edge fillet of 15 mm.

DESIGNED BY: Roselyn Kissaka DATE: NOVEMBER 2023	H ASSEMBLY		
CHECKED BY: Roselyn Kissaka DATE: NOVEMBER 2023			
SIZE A3	UNIVERSITY OF HERTFORDSHIRE		
SCALE 1:4	WEIGHT (kg) 2.95	LOCATION APPENDIX B	SHEET 2/4

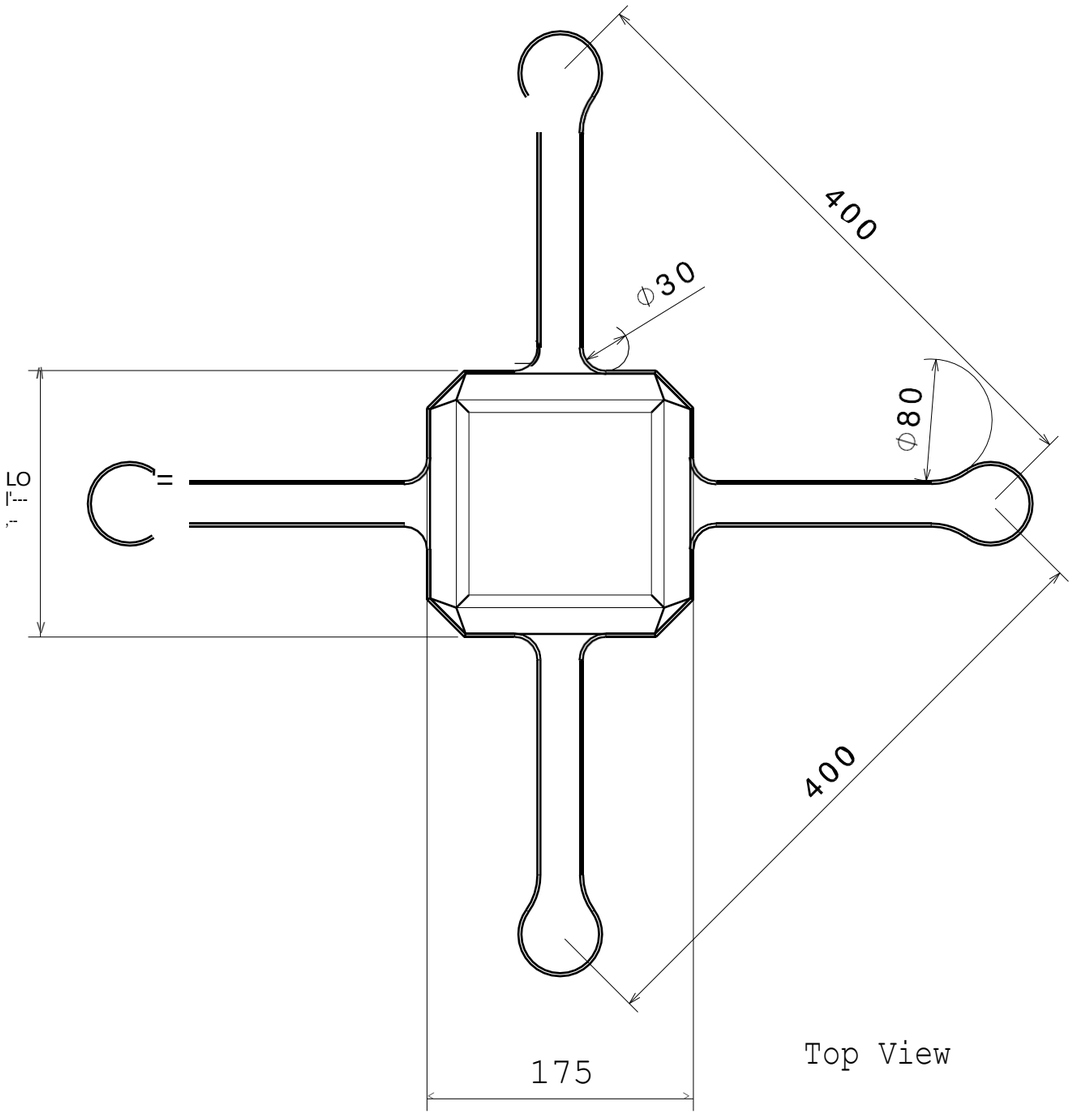

Top View

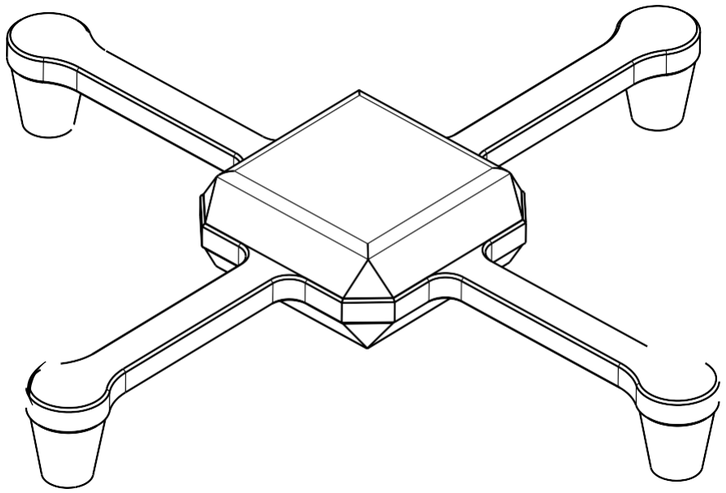

Isometric view
Scale: 1: 4

Part Number	Part Name
1	Top body part
2	Bottom body part
3	Plus middle layer
4	Quadcopter feet

NOTE:
1. The four faces on the top and bottom body parts have a face draft of 34 degrees.
2. The four corners on the top and bottom body parts, each have a draft of -17 degrees.
3. The middle layer with the arms has an edge fillet of 15 mm.

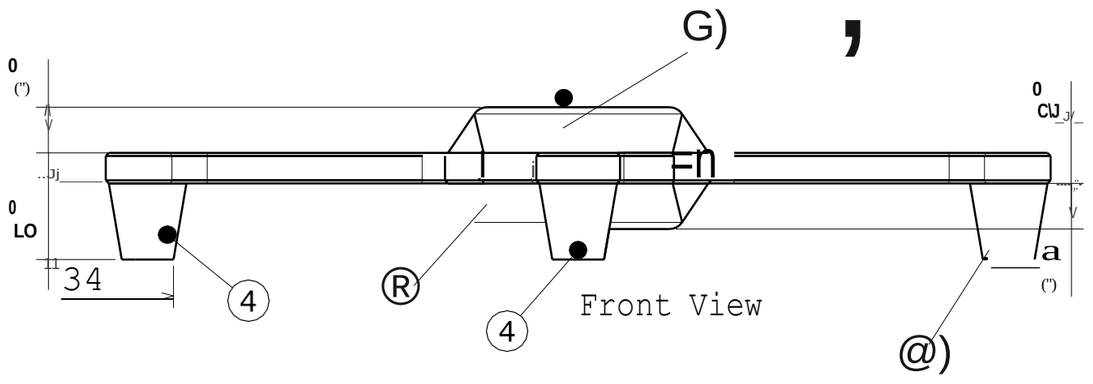

Front View

DESIGNED BY: Rasely Kissaka
DATE: NOVEMBER 2023
CHECKED BY: Roselyn Kissaka
DATE: NOVEMBER 2023

PLUS ASSEMBLY

smA3 | CJ©

UNIVERSITY OF HERTFORDSHIRE

SCALE	WEIGHT (kg)	LOCATION	SHEET
1 : 4	2. 82	APPENDIX B	3/4

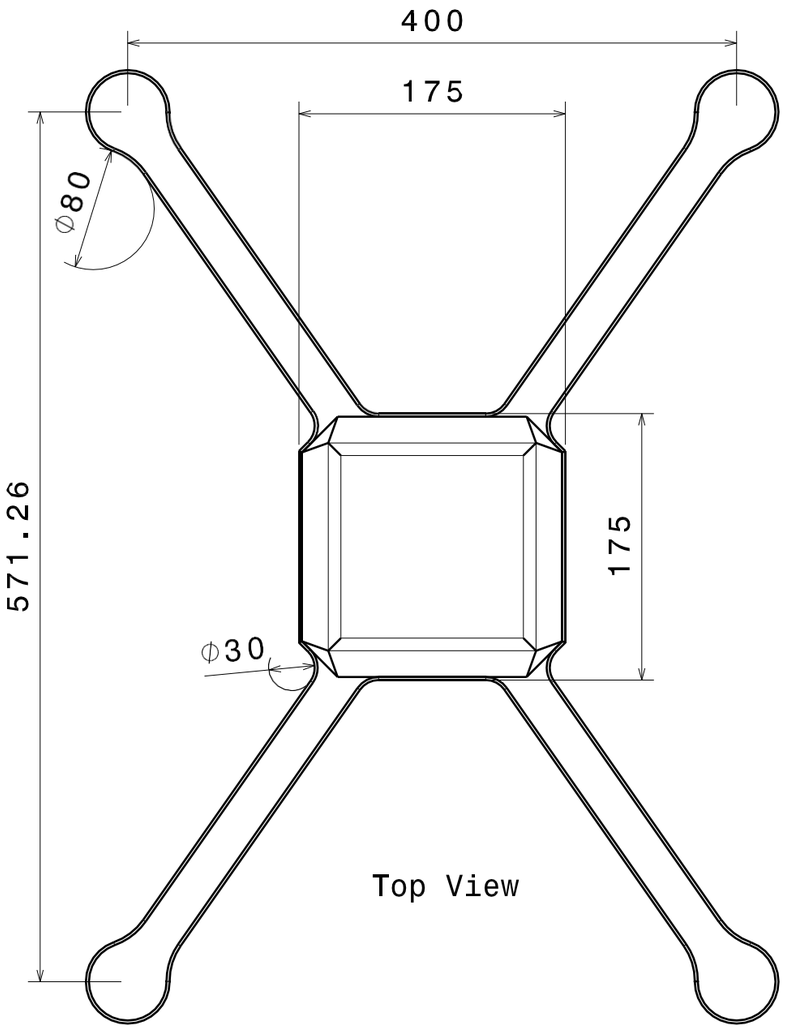

Top View

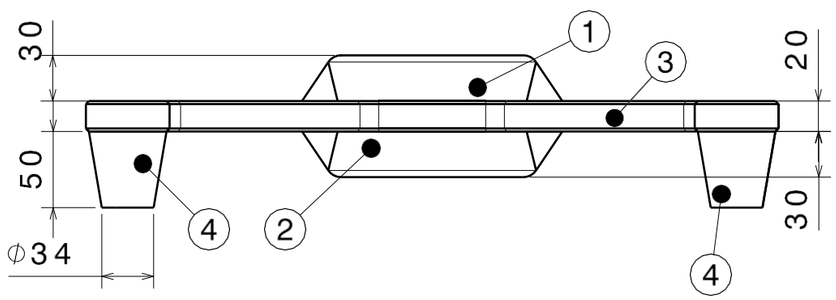

Front View

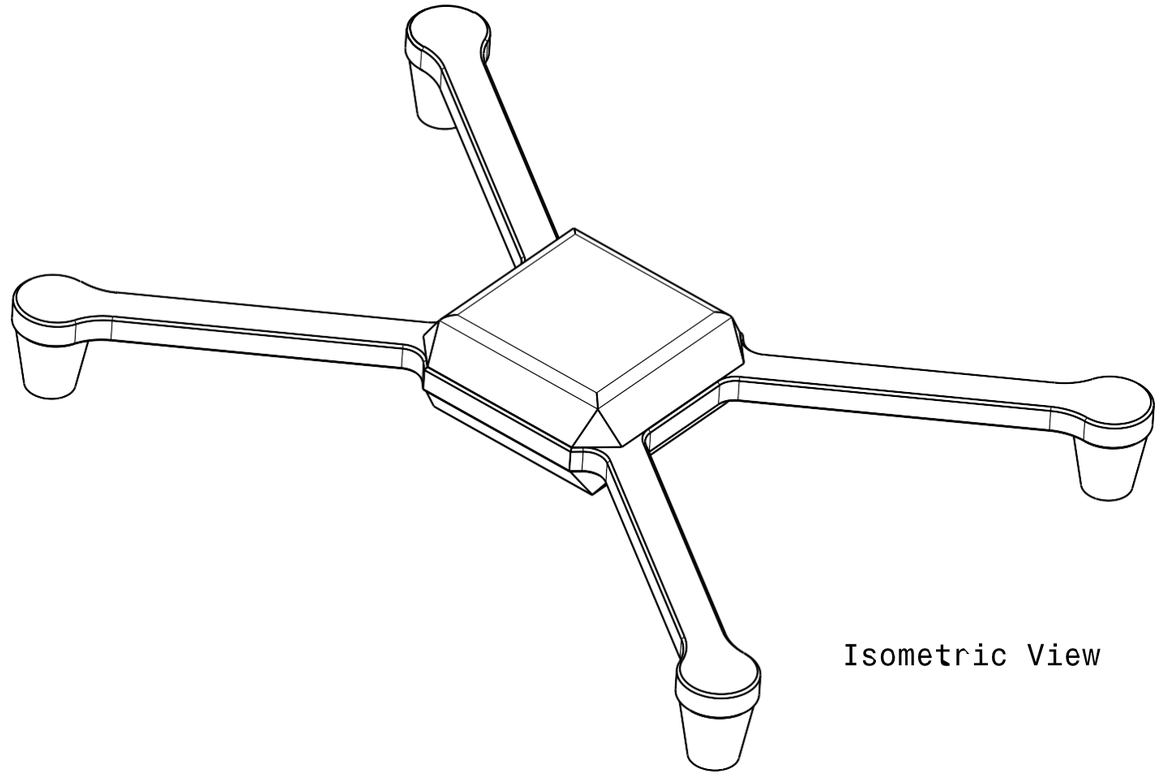

Isometric View

Part Number	Part Name
1	Top body part
2	Bottom body part
3	Plus middle layer
4	Quadcopter feet

NOTE:
1. The four faces on the top and bottom body parts have a face draft of 34 degrees.
2. The four corners on the top and bottom body parts, each have a draft of -17 degrees.
3. The middle layer with the arms has an edge fillet of 15 mm.

DESIGNED BY: Roselyn Kissaka DATE: NOVEMBER 2023	HYBRID X ASSEMBLY		
CHECKED BY: ROSELYN KISSAKA DATE: NOVEMBER 2023			
SIZE A3	UNIVERSITY OF HERTFORDSHIRE		
SCALE 1:4	WEIGHT (kg) 2.94	APPENDIX B	SHEET 4/4

I	H	G	F	E	D	C	B	A
_	_	_	_	_	_	_	_	_

ID	Task Name	Duration	Start	Finish
1	**INITIATON**	**22 days**	**Fri 29/09/23**	**Mon 30/10/2**
2	Initial Research	12 days	Fri 29/09/23	Sat 14/10/23
3	Defining aims and objectives	1 day	Mon 09/10/23	Mon 09/10/23
4	Resource Analysis	1 day	Tue 03/10/2	3Tue 03/10/23
5	Logbook Submissio	0 days	Sat 07/10/23	Sat 07/10/23
6	Project Outline Writing	14 days	Tue 03/10/23	Fri 20/10/23
7	Project Outline Review	1 day	Mon 23/10/23	Mon 23/10/23
8	Project Outline Submission	0 days	Mon 30/10/23	Mon 30/10/23
9	Internet search for CAD models	10 days	Mon 09/10/23	Fri 20/10/23
10	Logbook Submissio	0 days	Sat 14/10/23	Sat 14/10/23
11	**CAD DESIGNING**	**11 days**	**Mon 16/10/2**	**Sat 28/10/23**
12	**CATIA**			
13	Modeling True X configuration	7 days	Mon 16/10/23	Tue 24/10/23
14	Modeling Hybrid X configuration	7 days	Mon 16/10/23	Tue 24/10/23
15	Logbook Submissio	0 days	Sat 21/10/23	Sat 21/10/23
16	Modeling H cinfiguration	5 days	Mon 23/10/23	Fri 27/10/23
17	Modeling '+' Configuration	5 days	Mon 23/10/23	Fri 27/10/23
18	Logbook Submissio	0 days	Sat 28/10/23	Sat 28/10/23
19	**SIMULATION**	**89 days**	**Wed 11/10/2**	**Mon 12/02/2**
20	**STAR CCM+**	**48 days**	**Wed 11/10/2**	**Fri 15/12/23**
21	Practice and Tutorial 1	9 days	Wed 11/10/23	Sun 22/10/23
22	Practice and Tutorial 2	6 days	Mon 23/10/23	Mon 30/10/23
23	Defining and creating aerial conditions	1 day	Mon 23/10/23	Mon 23/10/23
24	Simulation on True X model	14 days	Wed 25/10/23	Mon 13/11/23
25	Simulation on Hybrid X model	14 days	Wed 25/10/23	Mon 13/11/23
26	Logbook submission	0 days	Sat 04/11/23	Sat 04/11/23
27	Simulation on H model	14 days	Tue 31/10/23	Fri 17/11/23
28	Simulation on '+' model	14 days	Tue 31/10/23	Fri 17/11/23
29	Logbook submssion	0 days	Sat 11/11/23	Sat 11/11/23

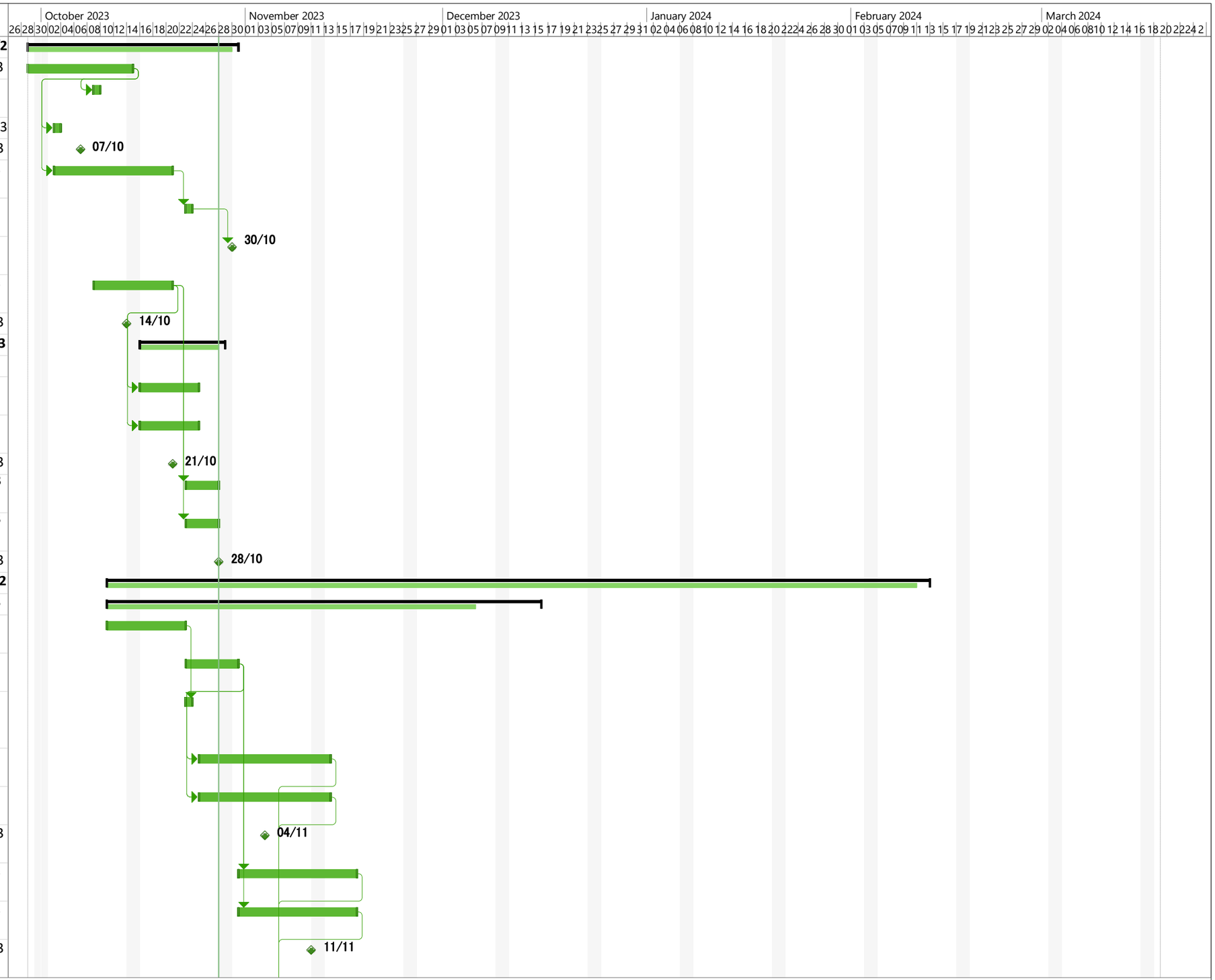

Project: Abel Ochieng Gantt c
Date: Sat 28/10/23

Task	Project Summary	Manual Task	Start-only	Deadline
Split	Inactive Task	Duration-only	Finish-only	Progress
Milestone	Inactive Milestone	Manual Summary Rollup	External Tasks	Manual Progress
Summary	Inactive Summary	Manual Summary	External Milestone

ID	Task Name	Duration	Start	Finish
30	Data Collection	9 days	Wed 08/11/2	Mon 20/11/2
31	Data Compariso	11 days	Tue 21/11/2	Tue 05/12/23
32	Logbook submission	0 days	Sat 18/11/23	Sat 18/11/23
33	**MATLAB**	**45 days**	**Mon 11/12/2**	**Sat 10/02/24**
34	Defining Parame	2 days	Mon 11/12/2	Tue 12/12/23
35	Internet search for mathematical models	4 days	Mon 11/12/23	Thu 14/12/23
36	Mathematical model simulation	5 days	Fri 15/12/23	Thu 21/12/23
37	Model modification	26 days	Fri 22/12/23	Fri 26/01/24
38	Logbook submission	0 days	Sat 13/01/24	Sat 13/01/24
39	Simulation on True X model	9 days	Mon 29/01/24	Thu 08/02/24
40	Simulation on Hybrid X model	9 days	Mon 29/01/24	Thu 08/02/24
41	Simulation on H model	9 days	Mon 29/01/24	Thu 08/02/24
42	Simulation on '+' model	9 days	Mon 29/01/24	Thu 08/02/24
43	Data collection	6 days	Mon 29/01/2	Mon 05/02/2
44	Data compariso	6 days	Mon 05/02/2	Sat 10/02/24
45	Logbook submission	0 days	Sat 10/02/24	Sat 10/02/24
46	**PROJECT CONCLUSION**	**30 days**	**Mon 05/02/24**	**Mon 18/03/24**
47	**Report Writing**	**30 days**	**Mon 05/02/2**	**Mon 18/03/2**
48	Report Introduction	11 days	Mon 12/02/24	Sat 24/02/24
49	Literature Review	11 days	Mon 12/02/24	Sat 24/02/24
50	Main Body	16 days	Mon 19/02/2	Sun 10/03/24
51	Conclusion	6 days	Fri 09/02/24	Fri 16/02/24
52	References and Appendix	6 days	Mon 11/03/24	Sat 16/03/24
53	Preperation of Presenation slides	11 days	Mon 05/02/24	Mon 19/02/24
54	Report Submission	0 days	Mon 18/03/24	Mon 18/03/24
55	Slides submissio	0 days	Mon 18/03/2	Mon 18/03/2

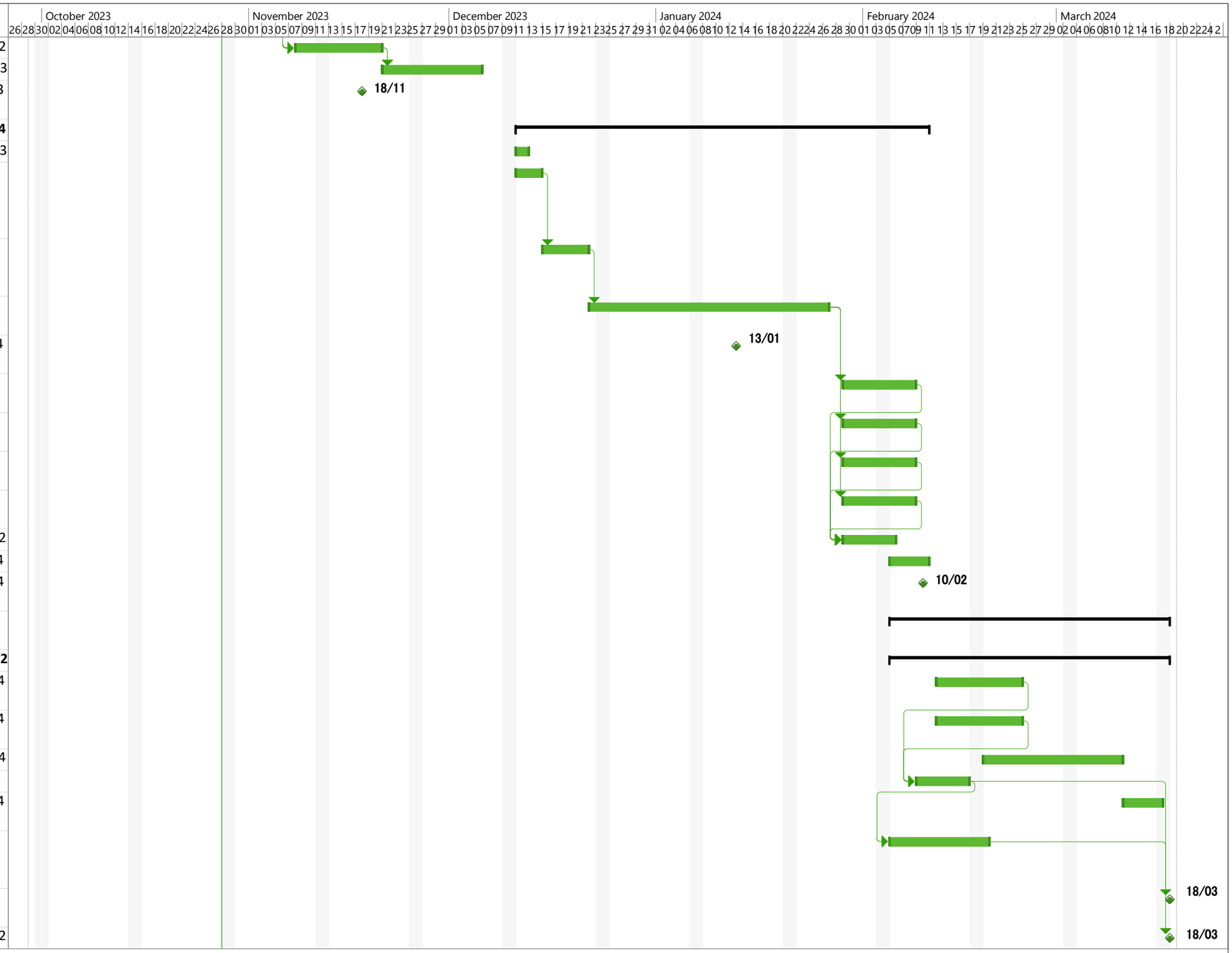

Project: Abel Ochieng Gantt c
Date: Sat 28/10/23

Task
Split
Milestone
Summary
Project Summary
Inactive Task
Inactive Milestone
Inactive Summary
Manual Task
Duration-only
Manual Summary Rollup
Manual Summary
Start-only
Finish-only
External Tasks
External Milestone
Deadline
Progress
Manual Progress

ID	Task Name	Duration	Start	Finish	Predecessors
1	**INITIATON**	**22 days**	**Fri 29/09/23**	**Mon 30/10/23**	
2	Initial Research	12 days	Fri 29/09/23	Sat 14/10/23	
3	Defining aims and objectives	1 day	Mon 09/10/23	Mon 09/10/23	2FS-5 days
4	Resource Analysis	1 day	Tue 03/10/23	Tue 03/10/23	2FS-9 days
5	Logbook Submissio	0 days	Sat 07/10/23	Sat 07/10/23	
6	Project Outline Writing	14 days	Tue 03/10/23	Fri 20/10/23	2FS-9 days
7	Project Outline Review	1 day	Mon 23/10/23	Mon 23/10/23	6
8	Project Outline Submission	0 days	Mon 30/10/23	Mon 30/10/23	7FS+4 days
9	Internet search for CAD models	10 days	Mon 09/10/23	Fri 20/10/23	
10	Logbook Submissio	0 days	Sat 14/10/23	Sat 14/10/23	
11	**CAD DESIGNING**	**26 days?**	**Mon 16/10/23**	**Sun 19/11/23**	
12	**CATIA**				
13	True X Design	6 days	Mon 16/10/23	Sun 22/10/23	
14	H Design	10 days	Mon 30/10/23	Fri 10/11/23	
15	Plus Design	10 days	Mon 30/10/23	Fri 10/11/23	
16	Hybrid X Design	6 days	Mon 23/10/23	Sun 29/10/23	
17	New True X Design	1 day	Sat 18/11/23	Sat 18/11/23	
18	New H Design	1 day	Sat 18/11/23	Sat 18/11/23	
19	New Plus Design	1 day	Sat 18/11/23	Sat 18/11/23	
20	New Hybrid X Design	1 day	Sat 18/11/23	Sat 18/11/23	
21	Logbook Submission	0 days	Sat 21/10/23	Sat 21/10/23	
22	Logbook submission	0 days	Sat 28/10/23	Sat 28/10/23	
23	Logbook Submission	0 days	Sat 04/11/23	Sat 04/11/23	
24	Logbook Submission	0 days	Sat 11/11/23	Sat 11/11/23	
25	Logbook Submission	0 days	Sat 18/11/23	Sat 18/11/23	
26	**CFD SIMULATION**	**109 days?**	**Wed 11/10/23**	**Sun 10/03/24**	
27	**Quadcopter models**	**109 days?**	**Wed 11/10/23**	**Sun 10/03/24**	
28	Practice and Tutorial 1	6 days	Mon 16/10/23	Sun 22/10/23	
29	Practice and Tutorial 2	6 days	Mon 23/10/23	Sun 29/10/23	28
30	Researching physical properties	6 days	Mon 23/10/23	Sun 29/10/23	
31	Defining physical properties	6 days	Mon 23/10/23	Mon 30/10/23	30FS-5 days
32	True X simulation using freestream	16 days	Tue 31/10/23	Tue 21/11/23	31
33	True X Simulation using block boundary	6 days	Mon 13/11/23	Sun 19/11/23	
34	Mesh analysis 1	11 days	Mon 20/11/23	Sat 02/12/23	
35	Mesh analysis 2	6 days	Mon 04/12/23	Sat 09/12/23	34
36	True X model simulation 1	6 days	Mon 11/12/23	Sun 17/12/23	
37	True X model Simulation 2	6 days	Mon 01/01/24	Mon 08/01/24	36FS+10 days
38	H model Simulation	16 days	Mon 08/01/24	Mon 29/01/24	37FS-1 day
39	Plus Model Simulation	11 days	Mon 22/01/24	Mon 05/02/24	38FS-6 days
40	Hybrid X Simualtion	11 days	Mon 29/01/24	Mon 12/02/24	39FS-6 days

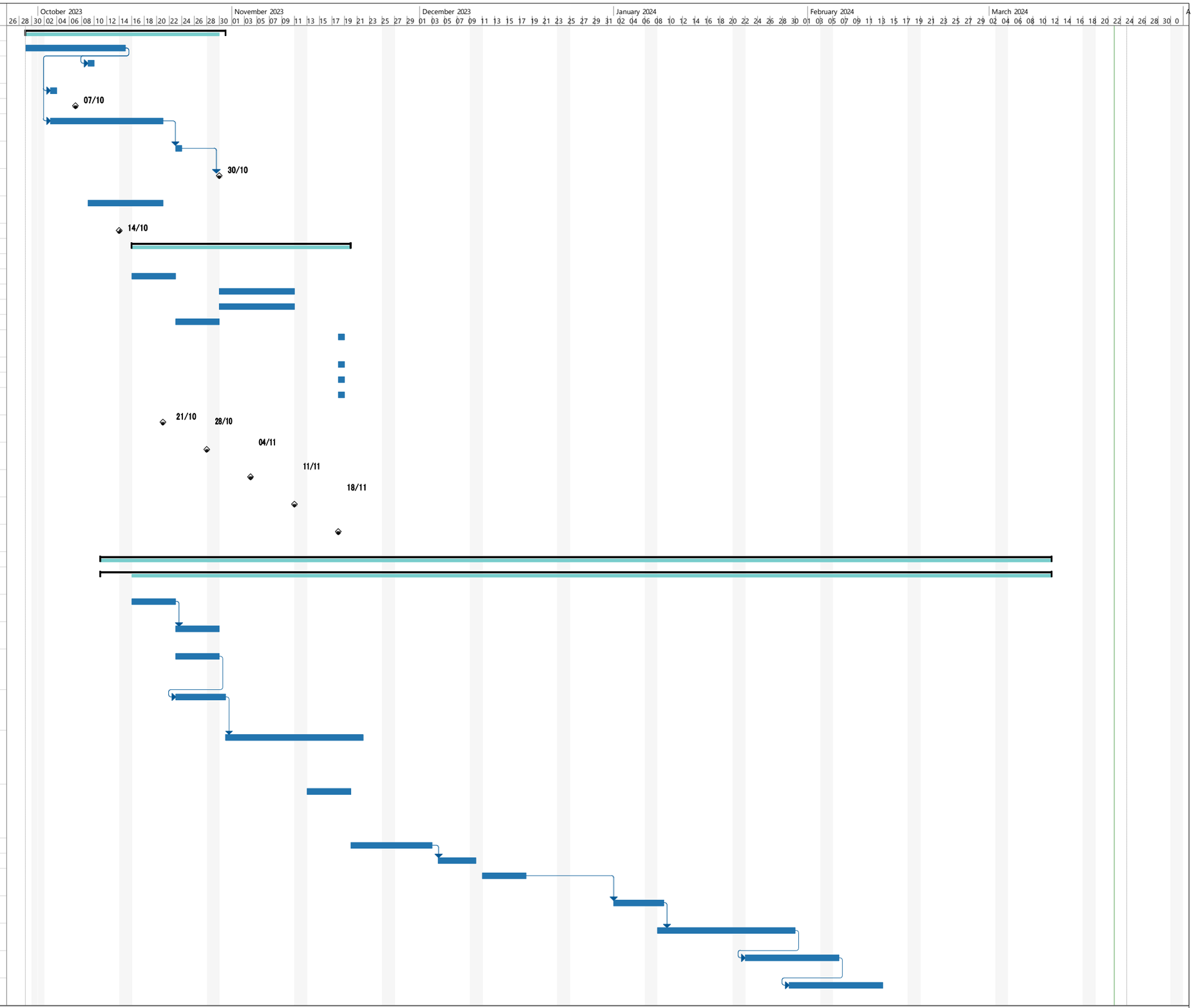

Project: Abel Ochieng Gantt c
Date: Thu 21/03/24

Task | Summary | Inactive Milestone | Duration-only | Start-only | External Milestone | Manual Progress
Split | Project Summary | Inactive Summary | Manual Summary Rollup | Finish-only | Deadline
Milestone | Inactive Task | Manual Task | Manual Summary | External Tasks | Progress

ID	Task Name	Duration	Start	Finish	Predecessors
41	Resimualtion of Plus model	11 days	Mon 26/02/24	Sun 10/03/24	
42	Data Compilation and comparison	11 days	Mon 19/02/24	Mon 04/03/24	41FS-15 days
43	Logbook Submission	0 days	Sat 25/11/23	Sat 25/11/23	
44	Logbook Submission	0 days	Sat 02/12/23	Sat 02/12/23	
45	Logbook Submission	0 days	Sat 09/12/23	Sat 09/12/23	
46	Logbook Submission	0 days	Sat 16/12/23	Sat 16/12/23	
47	Logbook Submisison	0 days	Sat 06/01/24	Sat 06/01/24	
48	Logbook Submission	0 days	Sat 13/01/24	Sat 13/01/24	
49	Logbook Submission	0 days	Sat 20/01/24	Sat 20/01/24	
50	Logbook Submission	0 days	Sat 27/01/24	Sat 27/01/24	
51	**Validation**	**96 days?**	**Mon 23/10/23**	**Sun 03/03/24**	
52	Search for Validation projects	6 days	Mon 23/10/23	Sat 28/10/23	
53	Design Validation models	6 days	Mon 12/02/24	Sun 18/02/24	
54	Flat plate simulation	6 days	Mon 19/02/24	Sat 24/02/24	
55	Bullet simulation	6 days	Mon 19/02/24	Sun 25/02/24	
56	Logbook Submission	0 days	Sat 03/02/24	Sat 03/02/24	
57	Logbook Submission	0 days	Sat 10/02/24	Sat 10/02/24	
58	Logbook Submission	0 days	Sat 17/02/24	Sat 17/02/24	
59	Logbook Submission	0 days	Sat 24/02/24	Sat 24/02/24	
60	Logbook Submission	0 days	Sat 02/03/24	Sat 02/03/24	
61	**PROJECT CONCLUSION**	**41 days**	**Thu 25/01/24**	**Fri 22/03/24**	
62	**Report Writing**	**41 days**	**Thu 25/01/24**	**Fri 22/03/24**	
63	Report Preparation	3 days	Thu 25/01/24	Sun 28/01/24	
64	Report Introduction	12 days	Fri 01/03/24	Sun 17/03/24	
65	Literature Review	11 days	Mon 04/03/24	Sun 17/03/24	
66	Main Body	14 days	Mon 04/03/24	Thu 21/03/24	
67	Conclusion	4 days	Mon 18/03/24	Thu 21/03/24	
68	References and Appendix	4 days	Mon 18/03/24	Thu 21/03/24	
69	Preperation of Presenation slides	9 days	Mon 11/03/24	Thu 21/03/24	
70	Logbook Submission	0 days	Sat 09/03/24	Sat 09/03/24	
71	Logbook Submission	0 days	Sat 16/03/24	Sat 16/03/24	
72	Report Submission	0 days	Fri 22/03/24	Fri 22/03/24	67
73	Slides Submission	0 days	Fri 22/03/24	Fri 22/03/24	69

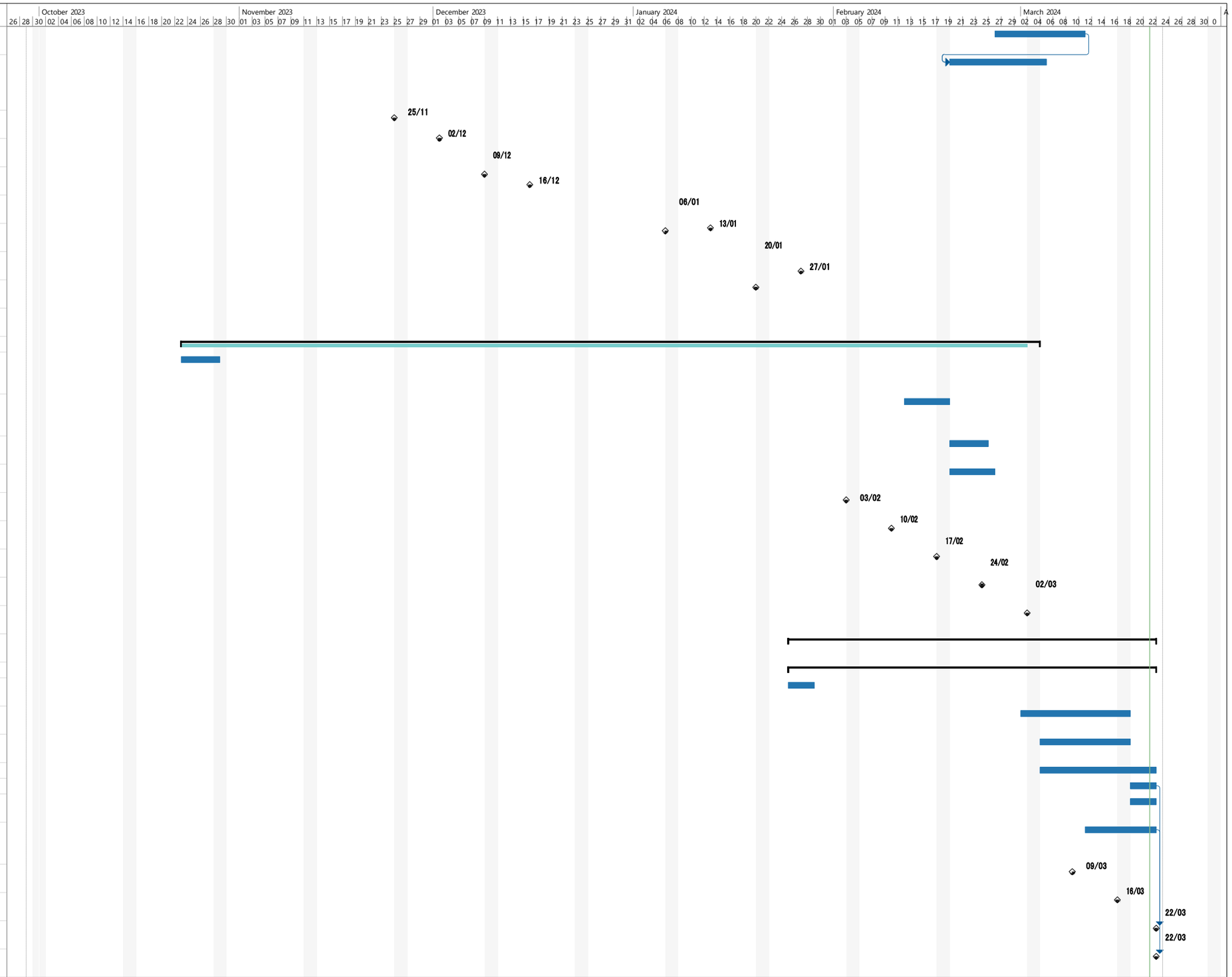

Project: Abel Ochieng Gantt c
Date: Thu 21/03/24

Task | Summary | Inactive Milestone | Duration-only | Start-only | External Milestone | Manual Progress
Split | Project Summary | Inactive Summary | Manual Summary Rollup | Finish-only | Deadline
Milestone | Inactive Task | Manual Task | Manual Summary | External Tasks | Progress